UNIVERSITY OF GAZİANTEP
GRADUATE SCHOOL OF
NATURAL & APPLIED SCIENCES

A NEW CONCEPT ON DESIGN OF HELICOPTER AND ROTOR

M. Sc. THESIS
IN
MECHANICAL ENGINEERING

BY
MEHMET HANİFİ DOĞRU
JULY 2012

A New Concept on Design of Helicopter and Rotor

M. Sc. Thesis
Mechanical Engineering
University of Gaziantep

Supervisor
Prof. Dr. İbrahim Halil GÜZELBEY

by

M. Hanifi DOĞRU

July 2012

T.C.
UNIVERSITY OF GAZİANTEP
GRADUATE SCHOOL OF
NATURAL & APPLIED SCIENCES
NAME OF THE DEPARTMENT

Name of the thesis: A New Concept on Design of Helicopter and Rotor
Name of the student: Mehmet Hanifi DOĞRU
Exam date: 13/07/2012

Approval of the Graduate School of Natural and Applied Sciences

Prof. Dr. Ramazan KOÇ
Director

I certify that this thesis satisfies all the requirements as a thesis for the degree of Master of Science.

Prof. Dr. L. Canan DÜLGER
Head of Department

This is to certify that we have read this thesis and that in our consensus opinion it is fully adequate, in scope and quality, as a thesis for the degree of Master of Science.

Prof. Dr. İbrahim.H. GÜZELBEY
Supervisor

Examining Committee Members	signature
Prof. Dr. İbrahim H. GÜZELBEY	
Prof. Dr. Naki TÜTÜNCÜ	
Asst. Prof. Dr. A. Tolga BOZDANA	

I declared that the related thesis is written properly according to academic and ethic rules and using all literature information referenced in the related thesis.

ABSTRACT

A NEW CONCEPT ON DESIGN OF HELICOPTER AND ROTOR

Mehmet H. Doğru
M. Sc. Thesis in Mechanical Eng.
Supervisor: Prof. Dr. İbrahim H. Güzelbey
July 2012, 58 pages

The purpose of this study is to eliminate one of the important problems of the helicopters. This problem is the created reverse torque on helicopters because of the rotation of the main rotor. The complicated and the detailed mechanism may be simplified and an alternative solution for the created reverse torque may be implemented. So, this thesis will concentrate on the innovative thoughts.

The calculation and the measurements of the created reverse torque are the primary tasks of this thesis. The static tapping system and the spring system are used to measure the reverse torque. The blade element theory is used to calculate the reverse torque. The validated torque from the calculation and measurements has been used to design a new anti-torque system.

The new anti-torque system has removed the tail part of an existing model helicopter. The tail rotor has been changed with a ducted fan. So a smaller, lighter and safer helicopter has been designed and constructed from the tail part point of view.

Key Words: Helicopter, Anti-Torque, Ducted Fan, Blade Element Theory

ÖZET

HELİKOPTER VE ROTOR TASARIMINA YENİ BİR YAKLAŞIM

Mehmet H. Doğru
Yüksek Lisans Tezi, Makina Mühendisliği
Danışman: Prof. Dr. İbrahim H. Güzelbey
Temmuz 2012, 58 sayfa

Bu çalışmanın amacı helikopter en önemli problemlerinden birini gidermektir. Bu problem helikopterin ana rotorunun dönüşünden dolayı oluşan ters torktur. Karmaşık ve detaylı mekanizmalar basitleştirilmiş ve oluşan ters tork için alternatif çözümler uygulanmıştır.

Oluşan ters torkun hesaplanması ve ölçülmesi bu tezin birincil görevidir. Bundan dolayı durağan basınç ve yay sistemi, ters torku ölçmek için kullanılmıştır. Ayrıca pala eleman teorisi de ters torku hesaplamak için kullanılmıştır. Ölçüm ve hesaplamalarla doğrulanan tork yeni anti-tork sistemi tasarımı için kullanılmıştır.

Yeni anti-tork sistemi var olan helikopterlerdeki kuyruk kısmını ortadan kaldırmıştır. Kuyruk rotoru kanal fanı ile değiştirilmiştir. Bundan dolayı daha küçük, hafif ve güvenli bir helikopter, kuyruk kısmına bakış açısından, tasarlanmış ve üretilmiştir.

Anahtar Kelimeler: Helikopter, Anti-Tork, Kanal Fan, Pala Eleman Teorisi

In memory of my Friend and Brother

Ediz ŞAVKIN

ACKNOWLEDGEMENTS

I wish to express my grateful appreciation to my supervisor Prof. Dr. İbrahim H. GÜZELBEY for his guidance, supports and encouragement.

I would like to thank my family and Nadide ÖZKUL for their love, care and prayers during this research.

I would like to acknowledge the contribution of Ediz ŞAVKIN who supported me with his friendship and help throughout this research.

I would also like to thank Prof. Dr. L. Canan Dülger, Asst. Prof. Dr. Ö. Yavuz Bozkurt and Asst. Prof. Dr.Emrah Özahi, İbrahim Göv and Kürşat Göv for their support.

CONTENTS

PAGE

LIST OF FIGURES

FIGURE **PAGE**

LIST OF TABLES

TABLE **PAGE**

Chapter 4

Chapter 5

LIST OF SYMBOLS

R_s	Radius of ducted fan exit (m)
V_∞	Free stream velocity (m/s)
V_s	Exit velocity of ducted fan (m/s)
A_s	Exit area of ducted fan (m^2)
V_{axial}	Axial velocity of blade (m/s)
$V_{angular}$	Angular velocity of blade (m/s)
V_{result}	Result velocity of blade (m/s)
r_p	Radius of propeller (m)
C_D	Drag coefficient
C_L	Lift coefficient
B	Number of blade
c	Chord length (m)
α	Angle of attack.
∅	Flow angle.
θ	Pitch angle
P	Absolute pressure (N/m^2)
v	Specific volume
R	Gas constant
T	Absolute temperature (K)
m	Mass (kg)
n	Number of moles
W	Mass flow rate (kg/s)
P_{atm}	Atmospheric pressure (N/m^2)
R	Temperature (K)
ρ	Density (kg/m^3)
Q	Volumetric flow rate (m^3/s)
U_{mean}	Mean velocity (m/s)
A	Duct area (m^2)

D	Diameter of duct (m)
r	Radius of duct (D/2) (m)
M	Mach number
a	Speed of sound (m/s)
g	Gravitational constant (m/s^2)
μ	Dynamic viscosity (kg/ms)
f	Darcy-weisbach friction factor
H_{loss}	Head loss due to friction (m)
H_{fan}	Head of the fan (m)
L	Between stating tapping measure (m)
z_1, z_2	Differences in between vertical position of static tapping (m)
k	Specific heat ratio of air
L_f	First length of spring (m)
L_e	Length of spring when spring is elongation situation (m)
Li	Distance of the moment test point to main gear (m)
x	Strain of spring (m)
k_{spring}	Coefficient of spring (N/m)
F_{spring}	Force of spring systems (N)
y, z	Measure between spring system and its moment axis (m)
T_{tail}	Tail rotor's produced torc (Nm)
T_{spring}	Thrust of spring systems (N)
$T_{static\ pressure}$	Thrust with static tapping systems (N)

ABBREVIATIONS

VTOL	Vertical take of landing
UAV	Unmanned aerial vehicle
CFD	Central fluid Dynamics
SEM	Scanning electron microscopy
AVA	Aviation vibration analyzer
NN	Neural-network
NREL	National renewable energy laboratory
BET	Blade element theory
MT	Momentum theory
CPR	Compressor pressure rules
RPM	Revolution per minute
NOTAR	No tail rotor
STS	Static tapping system
SS	Spring system
PC-GBS	Program ground base system
FDI	Fault detection and isolation
CPR	Characterization of performance responsible

CHAPTER 1

INTRODUCTION

1.1 GENERAL INTRODUCTION

A helicopter can be defined as a flying machine using rotating wings to provide lift, propulsion, and control forces that enable the aircraft to hover relative to the ground without forward flight speed to generate these forces. The thrust on the rotor is generated by the aerodynamic lift forces of the spinning blades. The rotation of rotor is obtained from the engine. It is the relatively low amount of power required to lift the machine compared to other vertical takeoff and landing (VTOL) machines that makes the helicopter unique. Efficient hovering flight with low power requirements comes about by accelerating a large mass of air at a relatively low velocity such as helicopters. In addition, the helicopter must be able to fly forward, climb, cruise at a high speed as much as possible, and then descend and come back to a hovering mode for landing. Of course these flight capabilities have a cost in terms of mechanical and aerodynamic complexity and higher power requirements. All of these factors have some influences on the design, acquisition, and operational costs of the helicopter [1].

A helicopter is an aircraft that is lifted and propelled by one or more horizontal rotors, each rotor consisting of two or more rotor blades. Helicopters are classified as rotorcraft or rotary-wing aircraft to distinguish them from fixed-wing aircraft [2].

The first flying attempt of human had been realized by Ibn Firnas in 9^{th} century. The second attempt had been done by Ismail ibn Hammad al-Cevheri. Those attempts had been collected, improved, reinvented and drawn by Leonardo da Vinci [3]. Later on Hezârfen Ahmed Çelebi had flown successfully [4]. All those real flying attempts may be considered as ornithopter concepts.

Igor Ivanovich Sikorsky was a Russian (later American) pioneer of aviation in helicopters. Sikorsky started in his vertical flight studies and tests in 1909 in Russia. In 1929, he applied to patent for his helicopter studies. Later on, His design plans eventually culminated in the first flight of the Vought-Sikorsky VS-300 in 1939 [3]. Time-line shows the development of helicopter until 1950 in the figure 1.1.

A helicopter can fly straight up or straight down, forward, backward, or sideways. It can even hover. Unlike most airplanes, helicopters can take off and land in a small space. In addition, they can fly safely at much slower speeds and lower altitudes than airplanes. However, they cannot fly as fast as most planes. Most helicopters cannot exceed 200 miles (320 kilometers) per hour. At faster flight speeds, the velocity of the rotor blade tips approaches the speed of sound, and it becomes difficult to rotate the rotor. At high speeds, strong vibrations also develop that could damage the blades. Helicopters also use more fuel than airplanes to travel the same distance. In general, helicopters can fly only two to three hours. [1]

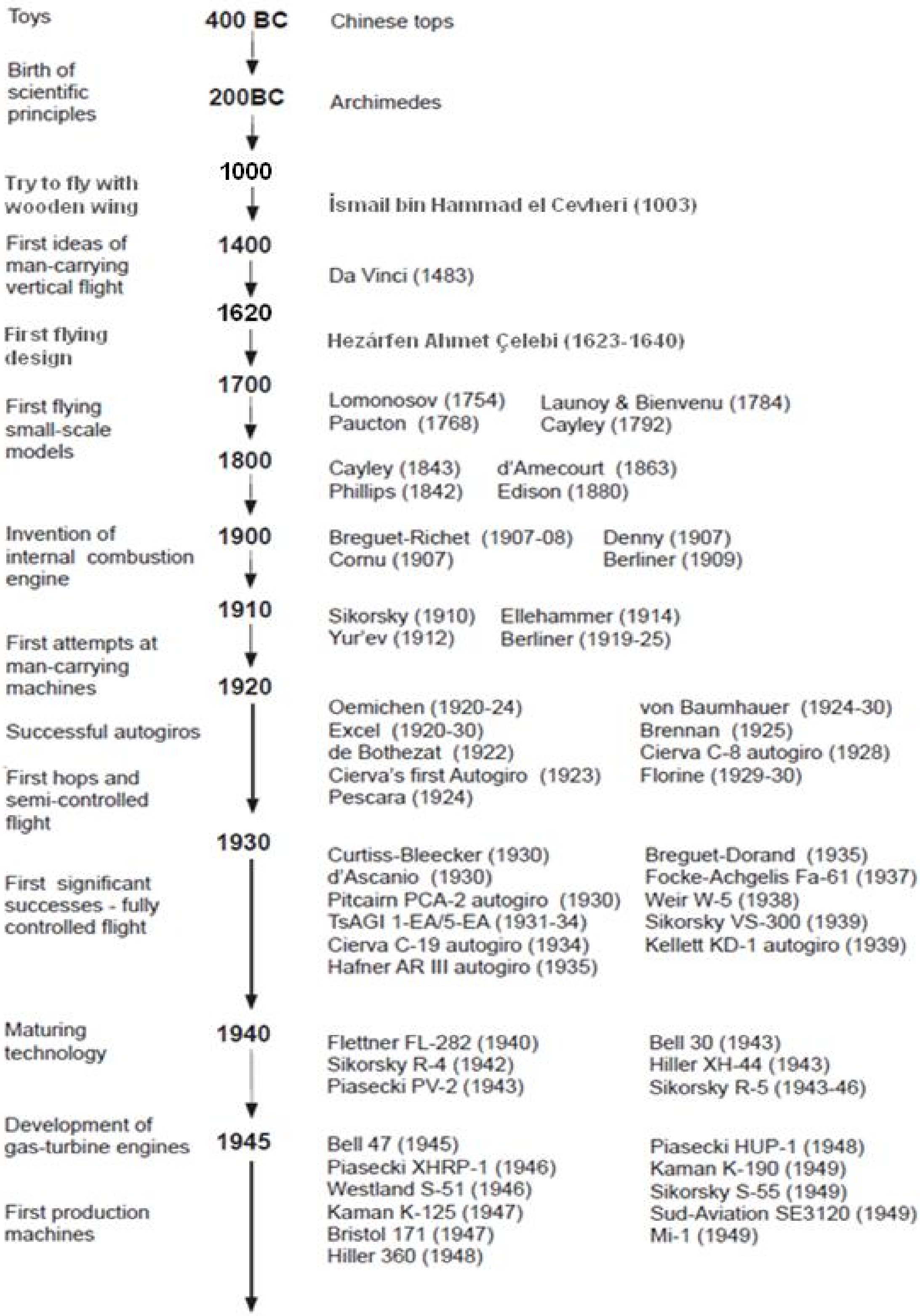

Figure 1.1 Improved Time-Line Showing Development of Helicopter and Autogiros Prior to 1950 [1]

1.2 RESEARCH OBJECTIVES and TASKS

In this thesis, the fundamental objective is investigated and developed helicopter and rotor systems. Helicopter is researched and studied for eliminating some problems. These problems are overcome with our new design. Research tasks can be summarized as follows:

1. Reviewing the helicopter and rotor systems in the literature.
2. The description of the created torque by main rotor
3. Using a suitable system to balance the created torque
4. Application to a model helicopter.
5. Validation of experimental and theoretical studies.

1.3 LAYOUT OF THESIS

A literature review about Helicopters, Rotor Systems, Design Concept and Analysis has been summarized in chapter two. Basic theory on helicopter and rotor is reviewed in chapter three. Air compressor is reviewed in chapter four. Design parameters are searched and added from literature. In the chapter five, the created torque and production of duct fan is studied. Case study is done in this chapter. In the chapter six, results and discussions are interpreted about thesis. In the chapter seven, conclusions have been given.

CHAPTER 2
LITERATURE SURVEY

2.1 INTRODUCTION

In this chapter, a summary of literature review which is related to helicopter rotors and other equipments is given. There are many problems in the control of helicopter due to two independent rotors. The helicopter has almost the most complex structure among aircrafts. In addition, the helicopter involves multidisciplinary work like structure, control, aerodynamic, mechanism and vibration.

2.2 STUDIES ON HELICOPTERS

Helicopters have been used in many fields, such as army, medical industry and transportation for years. In this respect, helicopters have been investigated only from structural point of view which is blade structure, fuselage structure and rotor structure by the researchers. In addition, there are many studies about aerodynamics of helicopter and dynamics of helicopter and materials of component of helicopter.

2.2.1 Flight Control of the Helicopters

A helicopter is a type of rotorcraft in which lift and thrust are supplied by one or more engine driven rotors. Many scientist and researchers have been investigating flight control of the helicopters for years. They have investigated different rotor types for controlling of the helicopter. Sergio et al. [5] tried to get the dynamical model of an original tri-rotor helicopter. The helicopter is created of three rotors with stationary pitch propellers; two fixed rotors turning in opposite directions and one rotor that can be tilted to control the yaw displacement. The roll and the forward displacement are controlled by using a nested saturations control law. The pitch and lateral displacement are controlled in a similar way. The nonlinear controller performance is tested on real experiments using a tri-rotor rotorcraft.

Tilt rotor is also a different rotor type which is either hovering or thrusting aircraft. This active control achieves with control structures and mathematical models. Song and Wang [6] studied the progresses of the research work on the designing flight control system. Flight control law of the tilt rotor aircraft is designed with the help of an inner/outer loop control structure and an eigenstructure assignment algorithm on the basis of a proper mathematical model already verified by the wind tunnel tests. The proposed control law has been born out through the construction of the flight control system and the flight tests.

Many researchers study for developing unmanned aircraft. Kemao et al. [7] presented the design and implementation of an autonomous flight control law for a small-scale unmanned aerial vehicle (UAV) helicopter. The approach is decentralized in nature by incorporating a newly developed nonlinear control technique, namely the composite nonlinear feedback control, together with dynamic inversion. The overall control law consists of three hierarchical layers, namely, the kernel control, command generator and flight scheduling. They are implemented and verified in flight tests on the actual UAV helicopter. The flight test results demonstrate that the UAV helicopter is capable of carrying out complicated flight missions autonomously.

2.2.2 Aerodynamics

Aerodynamics of helicopter must support two theories, which is momentum theory and blade element theory. The momentum theory is based on the laws of conservation of mass, momentum and energy and the blade element theory is basically the application of the standard process of aerofoil theory to the rotating blade. If the researchers do an optimization or analysis, they use basics of fluid dynamics. Flow characteristic is divided by two sections, which is laminar flow and turbulent flow. Many scientists studied on classification to flow speed like subsonic, transonic (sonic), supersonic and hypersonic.

Conlisk [8] discussed the fundamental aeromechanics of the wake and the flow on the blade and the primary methods of analysis, computation, and experiment employed to uncover the physics of the rotor wake are described. The helicopter rotor wake is among the most complex fluid dynamic structures being three dimensional and in many cases unsteady. The wake begins at the blades where the flow can be transonic near the blade tip and undergo compressible dynamic stall. Farther down in the wake, the flow is essentially incompressible. Moreover, the rotor blades undergo complex unsteady motions because of the necessity to balance moments; they are elastic as well.

While they are analyzing aerodynamics of helicopter, they use some of analysis program. This program can measure flow distance or flow characteristic. Chen et al. [9] presented results of the MSU TURBO simulations which show predicted range extension with stall control technology compared to measurements, and characteristics of the compressor flow field with and without stall control technology in this paper. All military and commercial gas turbine engine systems can benefit from the proposed work.

2.2.3 Design and Structure

For more years, many people have thought and designed an aircraft. They thought different type and style of helicopter. At first times, they designed simple models for flying, but when the helicopter fly, they noticed that something were false. While the time was going to forward, they faced many problems. So they improved their systems or designs. According to their thought, the most important design parameters were blade geometry and rotor type for helicopter. As they entered deep of helicopter systems, they had to build up some mathematical and geometrical equations and then they applied this equations and derivations their systems. In this manner, they developed more and more. Due to there is still design problems today, they do many determination of design parameter experiment.

Guowei et al. [10] presented a comprehensive design methodology for constructing small-scale UAV helicopters. The systematic design procedure, which includes hardware component selection, design and integration, as well as experimental evaluation, is utilized to construct a fully functional UAV helicopter, named SheLion. Various ground and flight tests have been performed to verify the feasibility and reliability of SheLion. This simple, systematic and effective methodology can be easily followed and used for building small-scale UAV helicopters for general research purposes.

Peter G. Hamel and Jiirgen Kaletka [11] described as the extraction of system characteristics from measured flight test data. Therefore it provides an excellent tool for determining and improving mathematical models for a wide range of applications. The increasing need for accurate models for the design of high bandwidth control systems for rotorcraft has initiated a high interest in and a more intensive use of system identification. The full range of identification approaches was applied to dedicated helicopter flight-test-data including data quality checking and the determination and verification of flight mechanical models. It was mainly concentrated on the identification of six degrees of freedom rigid body models, which provide a realistic description of the rotorcraft dynamics for the lower and medium frequency range.

Structure is almost the most important topic on an aircraft. Many researchers have studied to constitute a suitable material for aircraft because this material must be durable against temperature, pressure and vibration. Vibration causes fatigue on active or non-active parts on aircraft. Fatigue is most harmful situation for systems. Because of this vibration, scientists study to improve composite materials, which is sturdy against internal and external force. Separately lubricant systems are very important for aircraft systems. If lubricant systems don't operate truly, many parts may be damaged. As a result of this, failure may happen.

M. Balasko et al. [12] performed combined neutron- and X-ray radiography measurements at the Budapest Research Reactor. Several types of defects are detected, analyzed and typified. Among the most frequent and important defects observed are cavities, holes and/or cracks in the sealing elements on the interface of the honeycomb structure and the section boarders. In homogeneities of the resin materials (resin-rich or starved areas) at the core-honeycomb surfaces proved to be another important point. Defects are detected at the adhesive filling, and water percolation is visualized at the sealing interfaces of the honeycomb sections. Corrosion effects and metal inclusions have also been detected.

2.2.4 Analysis

Analysis is a matter that it is flagship of engineering. Many researchers use analyzing with different methods both design and experiment. While an aircraft is designing or producing, some of researchers or producers use analysis methods which are failure analysis, structural analysis, aerodynamic analysis, error analysis and so on. They use some analysis packet programs like Ansys, Abaqus or Pro-engineer. They improve their algorithms due to those commercial packages' results. They designed rotor type, blade geometry, control of helicopter, electrical systems of helicopter, fuselage type and analyzed the aerodynamics of helicopter and mechanics of helicopter using those softwares.

N.J. Lourenço et al. [13] analyzed the causes of a rupture which occurred with the main rotor grip device of a civil helicopter, which failed when the aircraft was attempting to land. From the visual examination of the fractured surface, it was possible to observe typical beach marks, thus indicating the occurrence of fatigue failure. Further examination, by using scanning electron microscopy (SEM) and metallography of the crack site, confirmed that the failure is caused by the mechanism of fatigue-crack initiation and growth from a corrosion pit located at the region of the blade retaining bolt hole.

Nathan A. Miller and Donald L. Kunz [14] conducted in order characterize the adjustment mapping of the Vibration Management Enhancement Program's PC-ground base system (PC-GBS), and compare it to the linear adjustment mapping used in the aviation vibration analyzer (AVA). Results show that, in a majority of situations, the neural network algorithms in PC-GBS produce adjustments that are identical to those produced by a linear algorithm similar to that used by AVA. Therefore, the use of neural networks for creating the mapping between adjustments and vibration response provides no significant improvement over a linear mapping.

D. McLean and H. Matsuda [15] presented the designs for a fuzzy-logic controller and neural-network (NN) controllers which are used to provide acceptable station-keeping performance for a single main rotor helicopter. The effectiveness of the proposed designs is established from an examination of a number of results obtained from a simulation of the controlled helicopter. The required training and recall data needed for the NN were obtained from there sponses of the same helicopter type being controlled in a station-keeping mode by a continuous, linear, optimal feedback control law, obtained by solving a linear quadratic regulator problem.

G. Heredia et al. [16] presented an actuator and sensor FDI system for small autonomous helicopters in this paper. Fault detection is accomplished by evaluating any significant change in the behavior of the vehicle with respect to the fault-free behavior, which is estimated by using observers. Several types of faults have been considered. The effectiveness of the proposed approach is demonstrated by means of experimental results and simulations.

M. Balasko et al. [17] performed to inspect the possible defects in the composite structure of helicopter rotor blades combined neutron- and X-ray radiography investigations at the Budapest Research Reactor. Imperfections in the honeycomb structure, resin rich or starved areas at the core-honeycomb surfaces, in homogeneities at the adhesive filling and water percolation at the sealing interfaces of the honeycomb sections were discovered.

2.2.5 Ducted Fan

In the literature, researchers have studied about propulsion systems and their analysis.

Aerodynamic performance of an aircraft propeller has been examined using the blade element and the momentum theory with vortex concept by Rwigema [18] and Wald [19]. The effects of blade tip modifications on a wind turbine blade have been carried out with an existing program which considers the curving of the blade axis in or out of the plane of rotation. The study is performed with a two-bladed rotor system with the NREL blade by Chattot [20].

A small aircraft powered by a ducted fan propulsion system has been developed by Ritschl et al. [21]. The proposed aircraft will be certificated in the ultra-light aircraft category.

Hence an analysis programming study have been carried out to provide an improved capability to existing software developed for estimating the performance of a ducted fan in a uniform axial flow. The capabilities have been added for modeling the center body, providing non-linear blade lift characteristics, calculating performance at very low advance ratios, calculation duct surface pressure distributions, and computing performance at angle of attack by Michael and Spangler [22].

On the other hand cross-flow fans give unique opportunities for distributed propulsion and flow control due to their potential for span-wise integration in aircraft wings. Cross-flow fan propulsion and flow control concepts have been studied by Dang and Bushnell [23].

A meaningful noise reduction can be achieved by reducing the diameter of a transonic propeller at constant rotational speed. The number of blades can be increased to obtain the required thrust. For this purpose, the blade element, a panel and Euler methods have been used. The blade element method has been involved into the work for the aerodynamic design and the panel method has been chosen for the aero-acoustic calculation. The inviscid panel method show that tip shape studies have little effects on noise but it affects efficiency directly by lieser et al. [24].

2.3 CONCLUSIONS

The literature review donated that there are many publications about helicopters. The few studies have focused on the controlling of the helicopter, analyzing the rotor shaft and rotor mechanism. But most of the researchers have been focused on the blade and the fuselage structure because of their simplicity. Investigations of control of helicopter and rotors may still require more works.

So our research will be focused on the following concepts:

1. The elimination of the complexity of the rotor mechanism.
2. The alternative and effective control for the helicopter.
3. The reduction of the weight of helicopter.
4. The independence of the control system from main rotor

CHAPTER 3

BASIC THEORY OF HELICOPTER AND ROTOR

3.1 INTRODUCTION

The helicopter is a kind of aircraft which is capable of vertical, horizontal, and stationary flight and high maneuver capability. Adversely they are more expensive to operate and difficult maintenance than aircrafts. The helicopter and its versatility have changed the daily life and combat tactics significantly. Moreover helicopters save lives, forests and money and can help to police and army [25].

3.1.1 How Helicopter Works

The principle of flight of an airplane, a bird, a rocket and a helicopter is based upon the aerodynamics rules. These rules are gravity, lift, drag, and thrust.

A helicopter flies by different methods than aircrafts. Its rotors and wings rotate in order to produce lift (Figure 3.1). In forward flight, this rotation is both hover and thrust the helicopter.

Figure 3.1 Blade Lift Effect [26]

Pilot can control the helicopter rotor systems with cyclic and collective (Figure 3.2). The cyclic lever is in front of the pilot and he uses to bank maneuver to left or right and to make the helicopter go forward or aft (backward).

Pilot has a collective, which is placed at left side of the pilot. The pilot uses the collective for increase or decrease velocity and ascends or descends the helicopter. The collective can also be considered as power control.

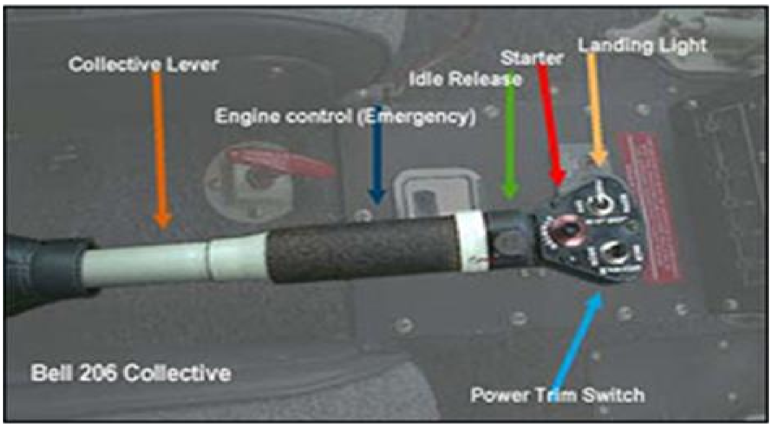

Figure 3.2 Collective [26]

The helicopter's tail rotor provides controlling of the helicopter's nose direction left or right. The tail rotor is controlled with foot pedals which are controlled by pilot. The tail rotors behave as a rudder on the helicopter.

When the main rotor blade rotates, they constantly change their pitch or angle of attack with cyclic and collective controls that is commanded by pilot (Figure 3.3). Angle of attack is an important concept to move the helicopter forward or backward.

Figure 3.3 Angle of Attack of Blade [26]

Helicopters generally use piston engines for source of power. Hence a gear box is used to transfer engine power into the main rotor and tail rotor. This is a special gear box named as combiner gear box [26].

3.1.2 Rotor Configurations

The common type of rotor is **a main rotor and a tail rotor** together. The tail rotor produces negative torque against main rotor. Pilots also use tail rotor to control vertical movements on the hover.

Tandem rotor is used in huge helicopter rotor systems. Basically two equal rotors produce equal power but in the opposite rotation aspect. So rotors will balance each other. Because of this system's complexity, control mechanism will be more complicated than the conventional helicopters which have a tail rotor. The control provided by rotor disc, which are bending against each other.

Two rotors side by side system is used in huge helicopter in early times. But because of these size, this system was never become a popular system.

Two rotors, comb into one another system works a gearwheel. One system returns to each other through. This system has not tail rotor because of one's produced torque is balanced by other rotor.

The coaxial rotor system has two rotors. One of the rotors is placed under the other one and it rotates in opposite direction. The lift difference between the two rotors is used to control vertical movement of helicopter. Helicopter's right or left turn depends on the torque difference between two rotors [27].

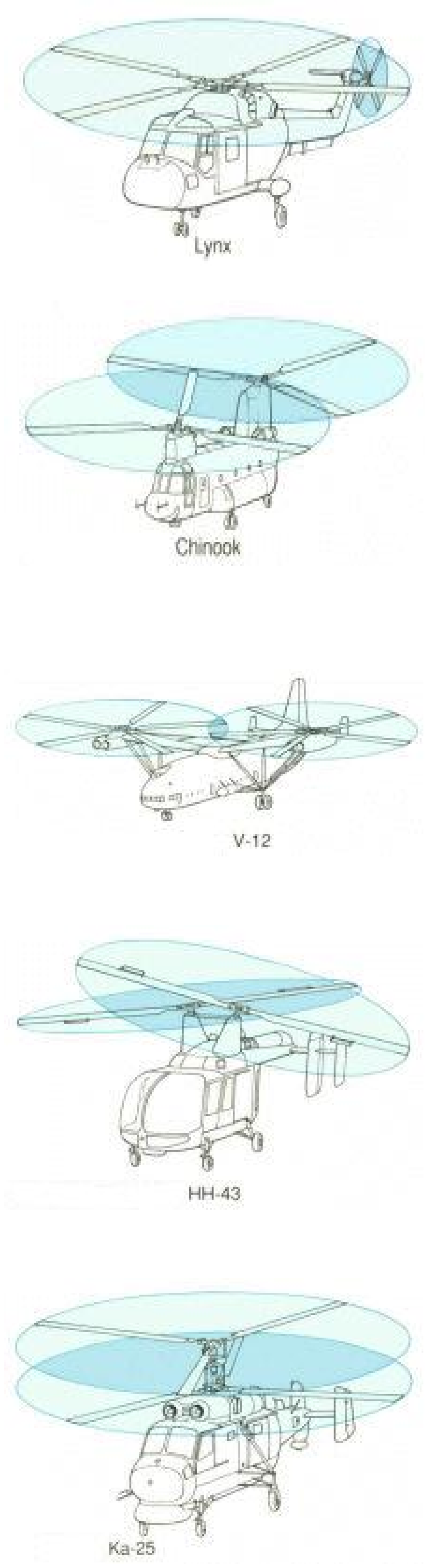

Figure 3. 4. Rotor Configuration [27]

3.1.3 Rotor Systems

Rotor systems have three rotor combinations most likely the fully articulated, rigid rotor systems and semi-rigid. (Figure 3-5).

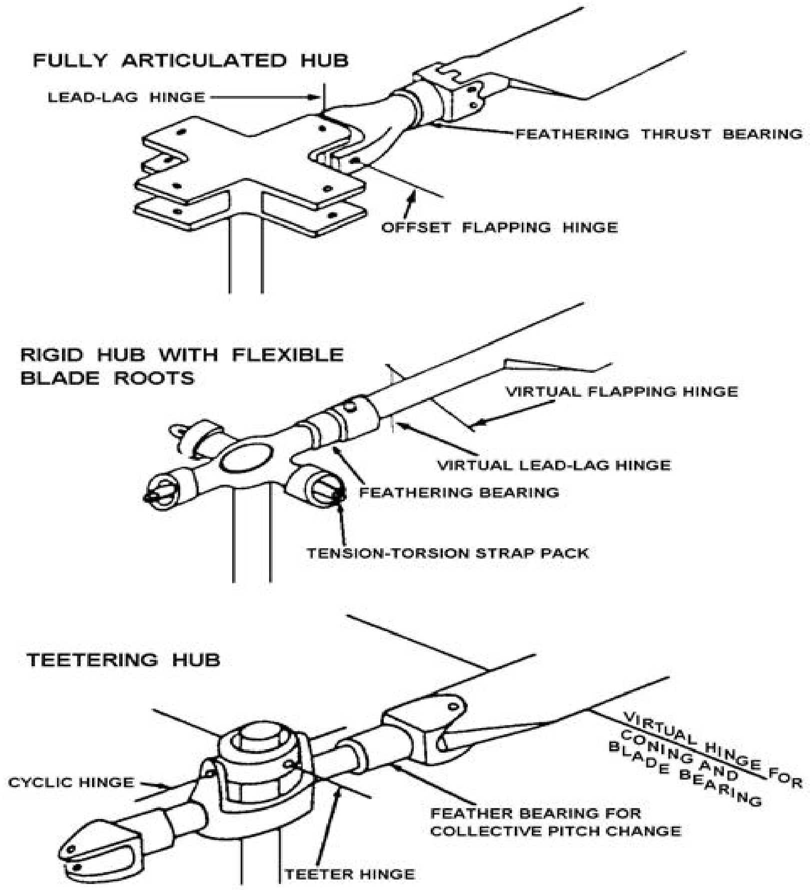

Figure 3.5 Rotor Systems [28]

More than two blades combine on the fully articulated rotor system. The lead-lag is enabled by vertical hinge pins. Each blade moves independently according to the rotor head.

Pitch control, flaps and hubs twist and bend to provide the lead-lag on the rigid rotor systems.

Two rotor blades are used in the semi-rigid rotor systems. Horizontal hinge pin is used for flapping independently. This system allows pitch movement [28]. Teetering hub rotor system is considered in this thesis.

3.2 BASIC THEORY ON HELICOPTER

3.2.1 Theories of Helicopter Flight

Helicopter aerodynamicists support two theories of helicopter flight: The Momentum Theory and the Blade Element Theory.

Blade element theory (BET) provides to find moments acting on a rotor blade and the aerodynamic forces in the forward flight. In this study, we applied blade element and momentum theory (MT) to describe the trust and torque of produced of helicopter main rotor.

Newton's investigation, which indicates that action and reaction principle, is the fundamental of the Momentum Theory. The mentioned action is the produced upward rotor trust and the reaction is the downward velocity in the rotor wake. The rotor thrust achieves the helicopter flight with total aerodynamic force produced in the rotor system.

The Momentum Theory adequately provides an explanation for no-wind, hovering flight, but it does not cover all of the bases. This is why we need BET.

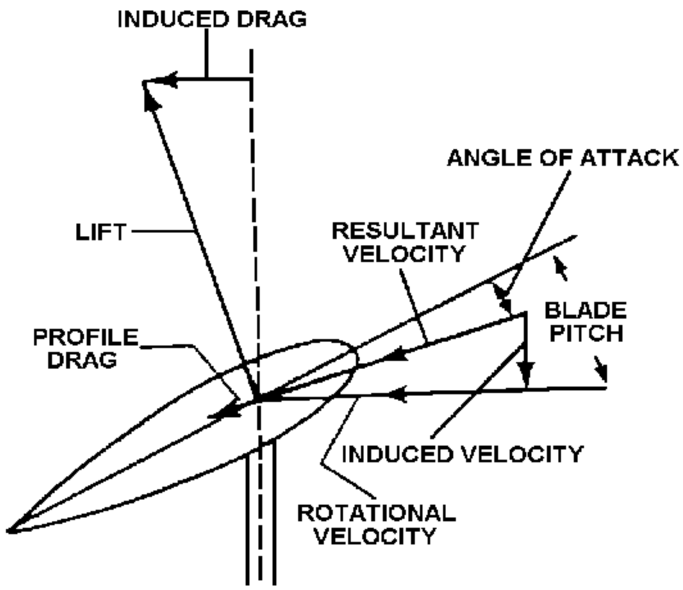

Figure 3.6 Blade Velocity Profile and Angle of Attack [28]

The Blade Element Theory is applied where the Momentum Theory is not reliable. Combination induced velocity and rotational velocity vectors are shown in the figure 3.6 [28].

3.2.1.1 Momentum Theory

The helicopter rotor produces an upward thrust by driving a column of air downwards through the structure of helicopter. A relationship between the produced thrust and the created velocity for the air can be obtained by the application of the laws of conservation of mass, momentum and energy to the overall process. This approach is commonly referred to the momentum theory. It corresponds essentially to the theory by Glauert for aircraft propeller which is based on earlier work by Rankine and Froude for marine propellers [29].

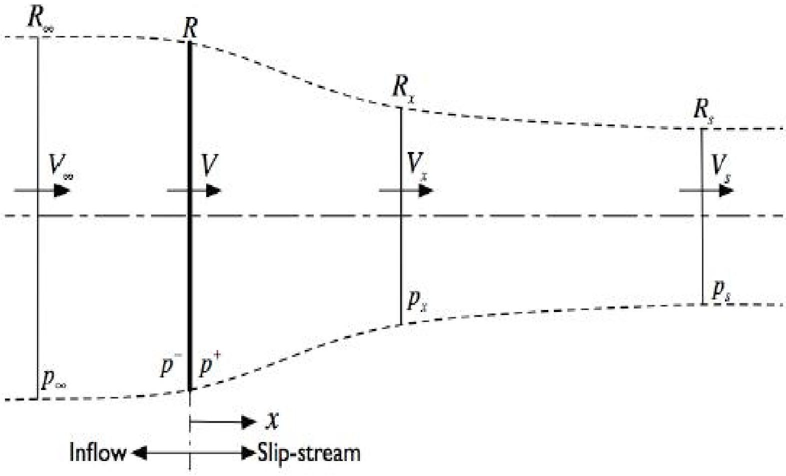

Figure 3.7 Propeller Stream Tube [18]

For the axial direction, the change in flow momentum along a stream-tube (Figure 3.7) must equal the thrust produced by the propeller.

$$T = \rho\pi R_S^2 V_S (V_S - V_\infty) \tag{3.1}$$

The conservation of mass is applied to the stream-tube control volume,

$$A_\infty V_\infty = A_S V_S = AV \tag{3.2}$$

For upstream, the static pressure is p_∞ and the velocity V_∞. The static pressure falls to a value p^- immediately upstream of the actuator disc and rises discontinnuously through the disc, to a value p^+ immediately downstream, although the velocity remains constant at V between these two planes, which are an infinitesimal distance apart. The thrust is therefore given by [18].

$$T = (p^- - p^+)A \tag{3.3}$$

3.2.1.2 Blade Element Theory

Blade element theory is basically the application of the standard process of aerofoil theory to the rotating blade. The blade is assumed to be rigid at normal rotational speeds so that the outward centrifugal force is the largest force acting on a blade and sufficient to hold the blade in rigid form. In vertical flight (including hover), the main complication is the need to integrate the elementary forces along the blade span. Offsetting this, useful simplification occurs because the blade incidence and induced flow angles are normally small enough to allow small-angle approximations to be made [29].

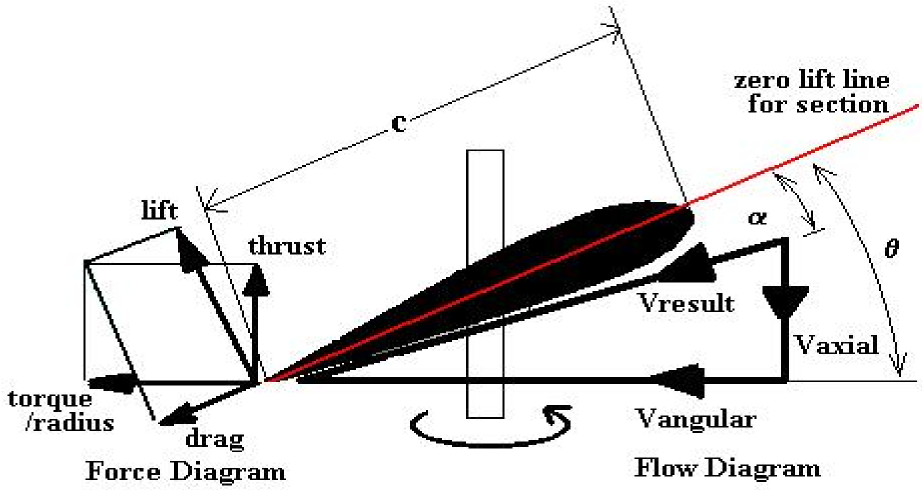

Figure 3.8 Blade Element Velocity Profile

Unless steady state of flow is assumed, momentum theory does not provide enough equations to solve for the differential propeller thrust and torque at a given span location. Blade element theory uses geometrical properties to determine the forces exerted by a propeller on the flow field. Lift and drag force consists of due to velocity flow (Figure 3.8). Propeller thrust is calculated using these equations [18].

Lift equation is,

$$\Delta L = C_L \frac{1}{2} \rho V_{result}^2 c.\,dr \tag{3.4}$$

Drag equation is,

$$\Delta D = C_D \frac{1}{2} \rho V_{result}^2 c.\,dr \tag{3.5}$$

Change in thrust is calculated,

$$\Delta T = \Delta L \cos(\emptyset) - \Delta D \sin(\emptyset) \tag{3.6}$$

$$\Delta T = \frac{1}{2} \rho V_{result}^2 c(C_L \cos(\emptyset) - C_D \sin(\emptyset)) B dr \tag{3.7}$$

CHAPTER 4

AIR COMPRESSORS

4.1 INTRODUCTION

In this chapter, a duct fan system is designed with a new concept rotor like a compressor. This fan system provides an anti-torque for balancing helicopter. This fan is used instead of the tail rotor. A torque meter is designed for calculating how much torque requires. All of these systems are manufactured and adapted in workshop of mechanical engineering.

4.2 GENERAL COMPRESSOR

Compressors are mechanical devices used to increase the pressure of air, gas or vapor. The inlet or suction pressure can range from low sub-atmospheric pressure levels to any pressure level compatible with piping and vessel strength limits. Compressor pressure ratio is defined as the ratio of the absolute discharge pressure to the absolute suction pressure.

Compression theory is primarily defined by the Ideal Gas Laws and the First and Second Laws of Thermodynamics. The Ideal Gas Law is based on the behavior of pure substances and takes the following form:

$$Pv = RT \tag{4.1}$$

Where

P = Absolute Pressure

v = Specific Volume

R = Gas Constant

T = Absolute Temperature

The ideal gas law can be manipulated to obtain several useful relationships. Both sides of the equation are multiplied by the mass "m" of the gas, the specific volume becomes total volume:

$V = mv$

$$PV = mRT \tag{4.2}$$

Considering that the mass of any gas is defined as the number of moles times its molecular weight

$m = n \times mw$

and

$$PV = n \times mw \times RT \tag{4.3}$$

and

$$\overline{R} = mw \times R \tag{4.4}$$

Where $\overline{R}$ is the universal gas constant

$$\frac{P_1V_1}{T_1} = n\overline{R} = mR = \frac{P_2V_2}{T_2} \tag{4.5}$$

Dividing both sides by time the total volume turns into volumetric flow and the mass flow per unit time turns into the mass flow rate W [30].

$$PQ = WRT \tag{4.6}$$

Where

W = Mass flow rate

Q = Volumetric flow rate

4.3 COMPRESSOR TYPES

Figure 4.1 indicates the two main compressor types: aerodynamic and displacement.

Displacement type compressors trap a certain amount of gas or air in a compression chamber and the volume is reduced mechanically. When the speed remains constant, the air flow also stays constant with the changes in the discharge pressure.

In dynamic type compressors, the impellers rotate at very fast and the energy caused by the high speed of impellers provides a continuous flow of gas or air. The energy caused by the high speed of impellers turns into pressure energy either by the diffusers or discharge volutes. In centrifugal type aerodynamic compressors, the relation between the head (or pressure) generated and the flow of air is determined by the geometry of the impeller.

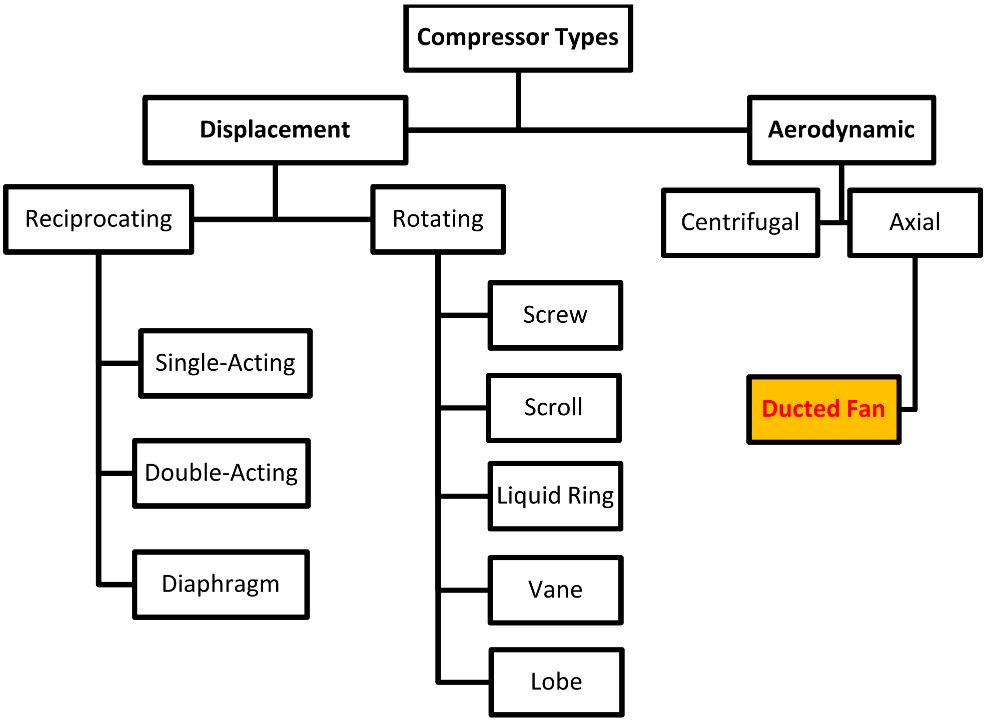

Figure 4.1 Compressor Types

4.3.1 Displacement Compressor

This type of compressors has two different types: rotary and reciprocating.

4.3.1.1 Reciprocating compressor

In figure 4.2 the shown reciprocating type of compressor is used widely in industrial applications for both refrigerant and air compressing purposes. They are characterized by the air or gas flowing out which stays approximately constant over the discharge pressure range and works with the principle of a bicycle pump. The output flow is pulsating and the capacity of the compressor is directly proportional to the velocity.

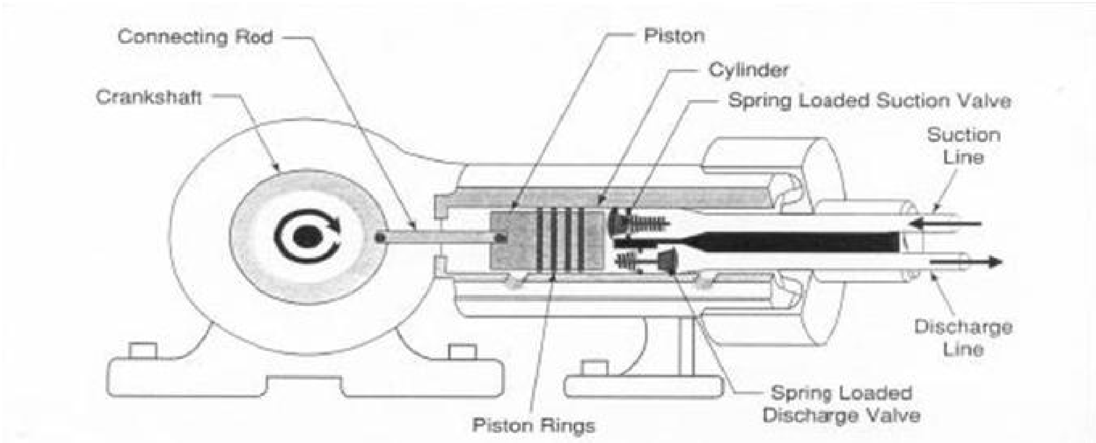

Figure 4.2 A Cross-Sectional View of a Reciprocating Compressor [31]

There are different variations of the reciprocating type compressors. Four most commonly used reciprocating type compressors are, vertical, tandem, horizontal, horizontal balance opposed. Single stage designed horizontal balance-opposed compressors operates at a capacity up to 10.000 cfm and multiple stage designed ones works in a range between 200 to 5.000 cfm. Hence the vertical types work in a capacity in between 50 to 150.

Reciprocating compressor types:

1. Single Acting
2. Double Acting
3. Diaphragm

4.3.1.2 Rotary compressor

Compressor rotor (Figure 4.3) is placed instead of pistons in the reciprocating type compressor, which give a continuous pulsation-free discharge. Rotary compressors work with high speeds and compared to reciprocating compressors rotary compressors give higher outputs. The rotary compressors are in compact size, light, easy maintainable and initial costs are low. Because of this reason they have a very wide use in industrial applications. The rotary type compressors are operated in the size ranges of 30-200 hp or 22-150 kW.

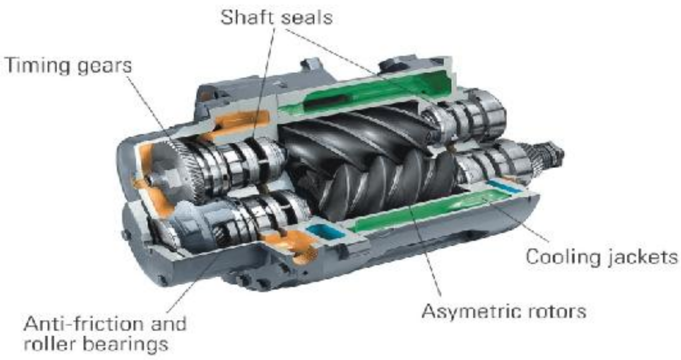

Figure 4.3 Rotary Compressor [31]

Types of rotary compressors:

1. Lobe
2. Screw
3. Vane
4. Scroll
5. Liquid Ring

4.3.2. Aerodynamic Compressors

4.3.2.1 Centrifugal Air Compressor

Figure 4.4 shows a view of a centrifugal type of air compressor. In this type of compressor, the impeller's rotational energy is transferred to air. They may be called as dynamic type compressor. The pressure and the momentum of air are changed by the rotor. The air enters into stationary diffuser and the momentum turns to a useful pressure. The centrifugal type air compressor is designed for oil-free usage. Atmospheric vents and shaft seals are used to separate the lubricated gear and the air.

The centrifugal type compressor works continuously. It does not contain many moving parts so that this type compressor is suitable for high volume applications.

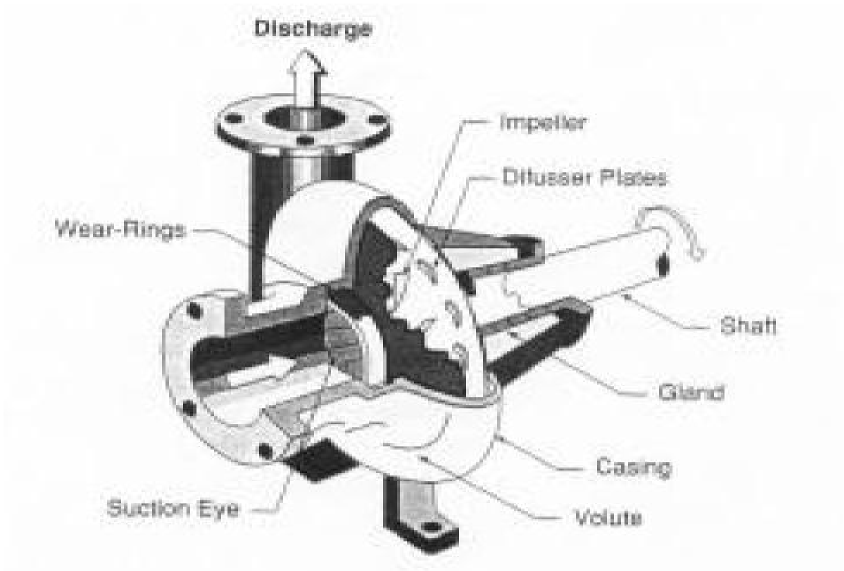

Figure 4.4 View of Centrifugal Compressor [31]

In high capacity applications centrifugal compressors are suitable. In the following table 4.1 the selection criteria of compressors are listed according to the type of application. [31]

Table 4.1 General Selection Criteria of Compressors [31]

Type of Compressor	Capacity(m^3/h)		Pressure (bar)	
	From	**To**	**From**	**To**
Roots blower compressor single stage	100	30000	0.1	1
Reciprocating				
-Single/two Stage	100	12000	0.8	12
-Multi Stage	100	12000	12.0	700
Screw				
-Single Stage	100	2400	0.8	13
-Two Stage	100	2200	0.8	24
Centrifugal	600	300000	0.1	450

4.3.2.2 Axial Air Compressor

The air flow and the rotational axis are parallel in the axial type compressors. Several rows of airfoil cascades compose the compressor. These rows are called as rotors. Rotors are connected to a central main shaft and rotate with high speed. Stators are the other rows which are stationary. The stators are responsible of the pressure increase. Hence the spiraling of air flow around the shaft is prevented by stators by making the flow parallel to the axis back. Figure 4.5 shows a computer modeled axial type compressor with stators and rotors. The axial compressor is connected to the shaft which gets the power from the turbine situated at the end of the blue shaft.

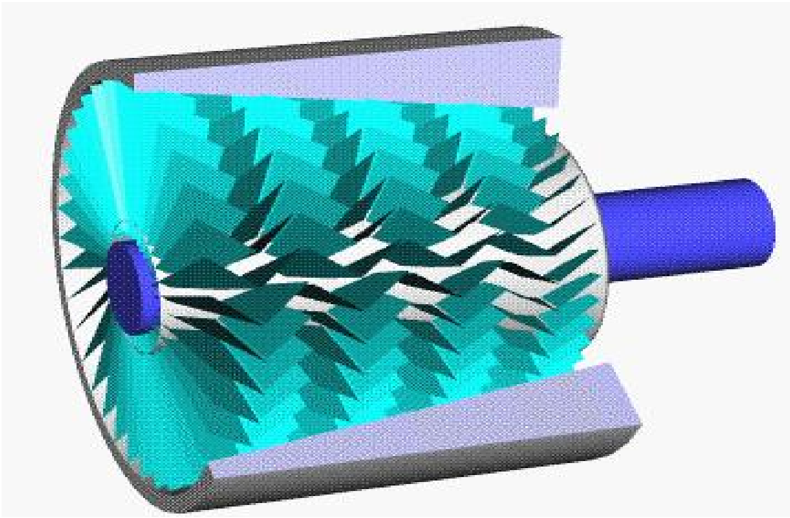

Figure 4.5 Axial Compressor [32]

The blades on stator or rotor create a pressure difference like an airfoil of a spinning propeller. The unsteady flow variations are created by continuously passing of the compressor blades around the upstream blade wakes. In a compressor design the designer should determine the axial type compressor performance by using wind-tunnel test and some advanced computational models. The ratio of the pressure across the compressor CPR is responsible of characterization of the performance. It is necessary that the shaft’s rotational speed to produce the increase in pressure and the factor of efficiency shows how much additional study has to be done related to an ideal axial compressor. [32]

CHAPTER 5

EXPERIMENTAL SETUP AND CASE STUDY

5.1 CREATED TORQUE BY MAIN ROTOR

5.1.1 Introduction

The rotation of main rotor creates turning moment. If this moment has not been balanced, helicopter turns around own axis. An experimental setup has been designed and constructed to determine the moment like a tail rotor, NOTAR (No Tail Rotor) and Fenestron systems.

A system was designed to learn how much force needs to balance moment of main rotor. The system is produced with bearing. All of these components were produced in mechanical engineering workshop without roller-bearing.

5.1.2 Production Steps

Firstly, a suitable system is designed to calculate force in tail rotor. It needs to calculate moment. It is manufactured according to test helicopter geometry.

A steel rod is used for stage shaft (Figure 5.1) and shaft (Figure 5.2). They are generated on turning machine.

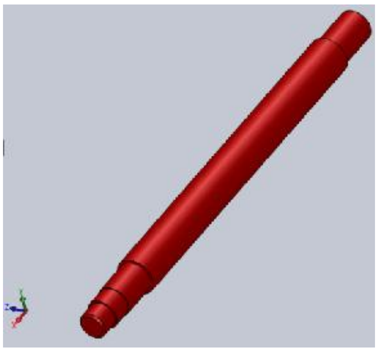

Figure 5. 1 Stage Shaft

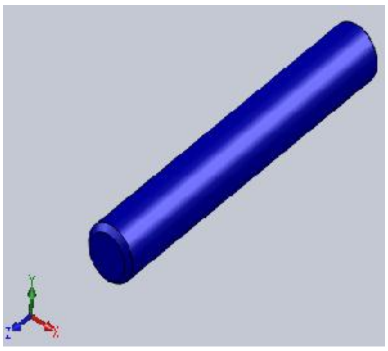

Figure 5. 2 Shaft

A tackle system is utilized for sliding yarn (Figure 5.3). It is taken from photocopying machine sliding systems. A metal plate is used to fix helicopter (Figure 5.4).

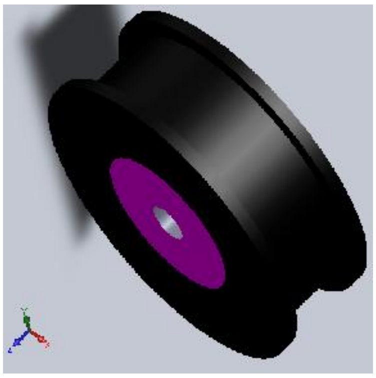

Figure 5. 3 Tackle

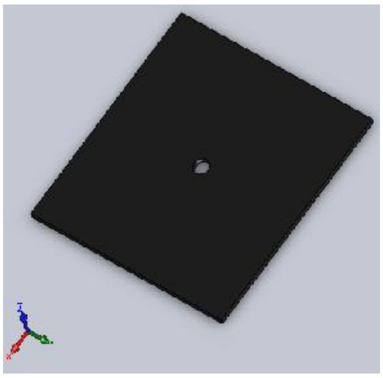

Figure 5. 4 Upper Plate

Two ball-bearing (Figure 5.5) and two bearing (Figure 5.6) are used for bearing the upper plate. Then, the helicopter is placed on this plate.

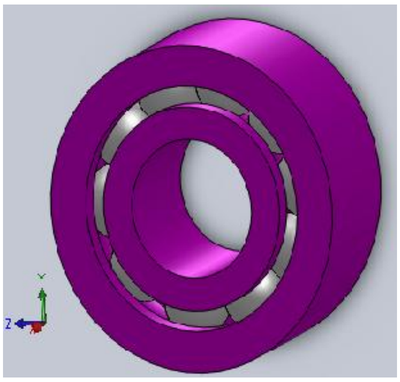

Figure 5. 5 Ball-Bearing

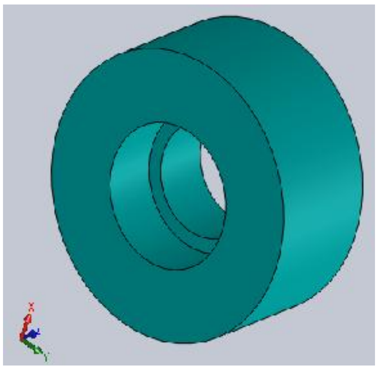

Figure 5. 6 Bearing

A carrier system (Figure 5.7) is hung on the yarn. Some weights (Figure 5.8) are added the carrier system. Then the measurement is taken from sensitive scale.

Figure 5. 7 Carier

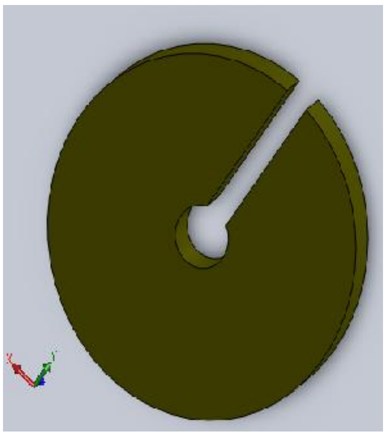

Figure 5. 8 Weight

In the figure 5.9, the sensitive scale is utilized for calculation tensile force. Its precision is 0,1 gram and the capacity of sensitive scale is 3000 gram.

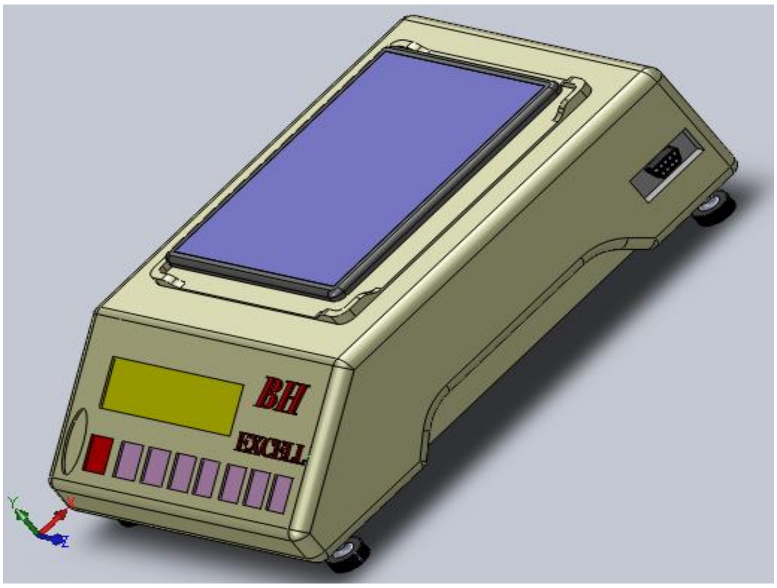

Figure 5. 9 Sensitive Scale

In the figure 5.10 and figure 5.12, isometric view of body is shown. All of these equipments are established on the body (Figure 5.11).

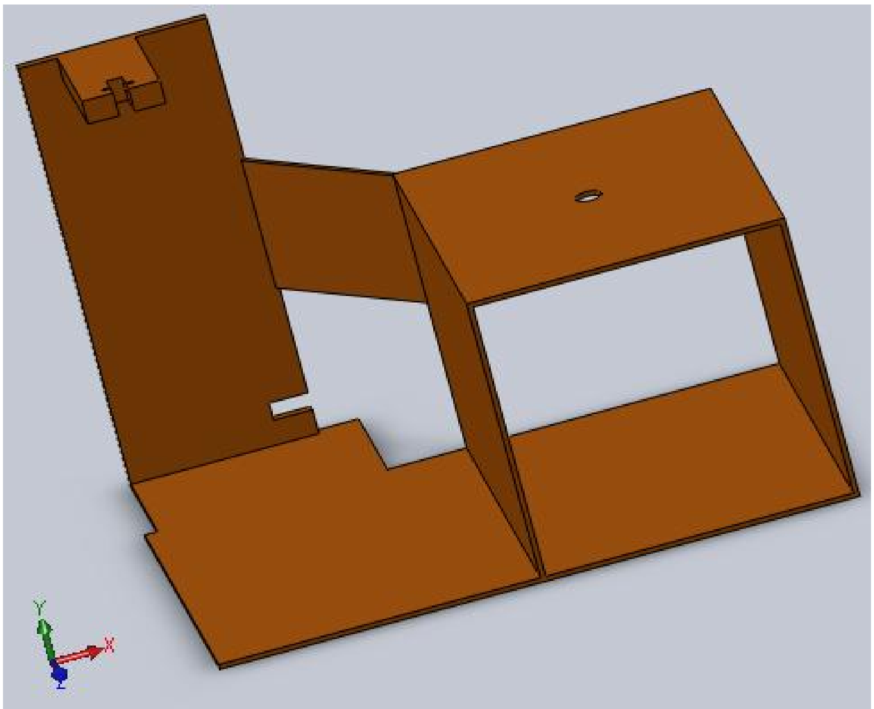

Figure 5. 10 Body

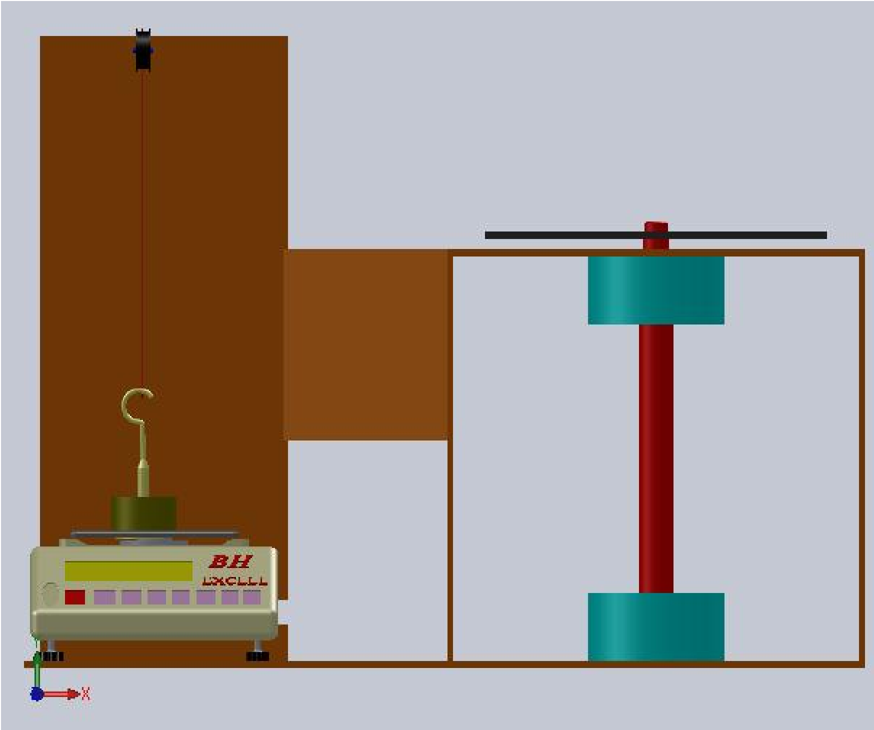

Figure 5. 11 Torque-meter Assembly-1

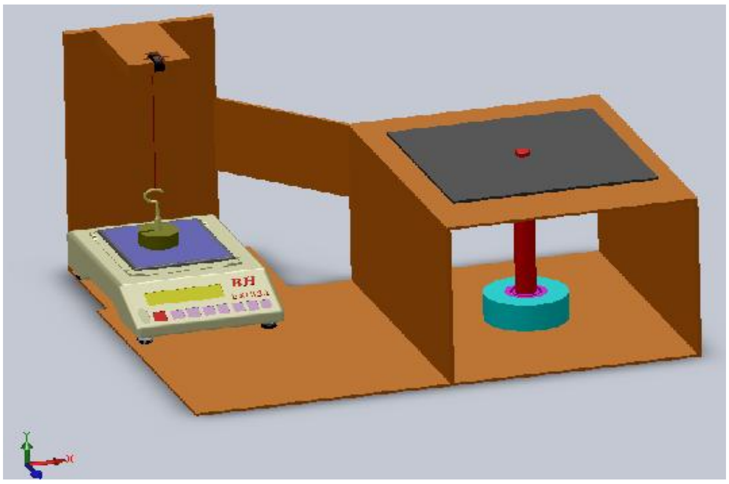

Figure 5. 12 Torque meter Assembly-2

5.1.3 Evaluation of the Helicopter Torque

Firstly, the helicopter is placed on the upper plate. Then, it is fixed using four screws on the upper plate. Tail shaft is stuck with a collar from A point (Figure 5.13 and Figure 5.14). A tip of yarn is connected from A point and other point of yarn is connected to carrier. 300 grams weights (total weights) are placed on the carrier.

When the helicopter is operated then the tail shaft is started to hold weights. Meanwhile, the lifting amount is read from indicator of sensitive scale. This test is repeated 20 times different dates and circumstances. The measurement values are in the table 5.1. The biggest measurement value is 0,1 kilograms.

Table 5. 1 Tail Rotor Holding Weight.

Test No	**Weight(gram)**	**Test No**	**Weight(gram)**
1	98.5	11	99.6
2	98.8	12	99.5
3	99.3	13	99.7
4	98.7	14	99.5
5	99.2	15	99.3
6	100	16	99.4
7	97.4	17	98.1
8	97.6	18	98.4
9	98.0	19	98.5
10	97.7	20	98.3

5.1.3.1 Calculation of the Torque

Newton's second law (Equation 5.1) is used for calculation the torque.

F=Force,
m=Mass,
a= Gravitational Acceleration Constant = 9.80665 m/s^2

$$\mathrm{F} = \mathrm{m} \times \mathrm{a} \tag{5.1}$$

A yarn is attached the tail shaft from A point. The distance between A point and main shaft measurement is X=0.275 m in the figure 5.13.

$$F=0.100\times9.80665=0.980\ kgm/s^2$$
$$=0.980\ N$$

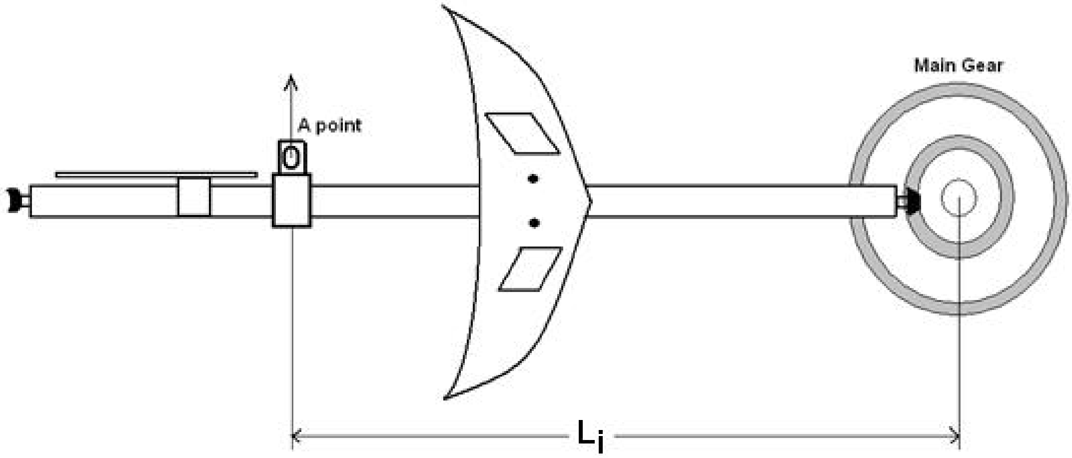

Figure 5. 13 Torque meter Tail Mechanism

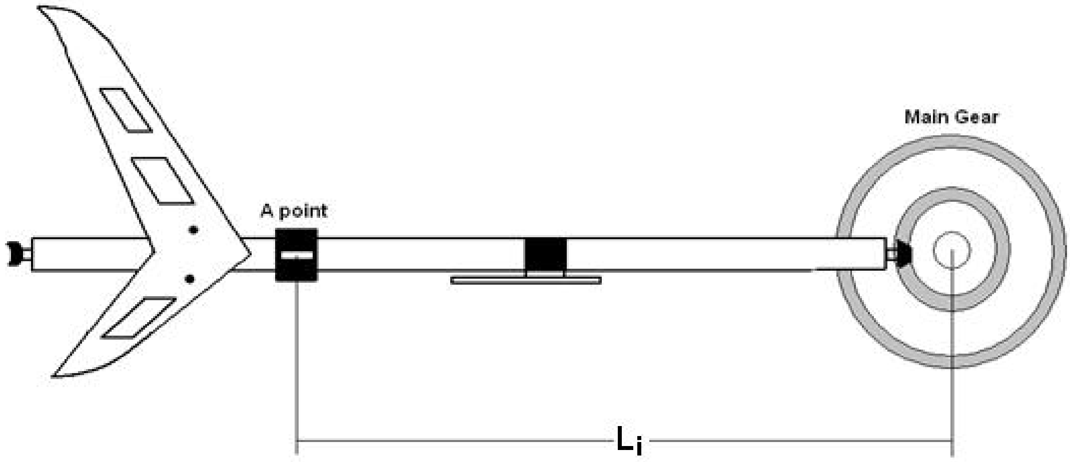

Figure 5. 14 Torque meter Tail Mechanism

Torque calculation formula is utilized with force and length and computed the necessary torque for balancing the helicopter in the equation 5.2.

T_{tail}=Torque,

Li=Distance of the moment test point to main gear,

$$T_{tail}=F\times Li \tag{5.2}$$

$$=0.980\times0.275$$

$$=0.2695\ Nm$$

5.2 DUCTED FAN

5.2.1 Introduction

When axial fans are not capable of producing high pressure, they are convenient for the application of handling high volumes of air relatively to low pressures. In common they have low prices and operate with good efficiency. Most of these fans have large hugs and may have the blades in the shape of an airfoil. Generally the blades are not close to each other, they may be produced in many different shapes. The most efficient blades have the similar sections of airfoil. Angle change is given to the blade at varying positions from hub to tip twist. The air is generally directed and aligned into the fan blades by the usage of inlet guide vanes which imparts energy to the air coming in.

Axial type fans are efficient and can work in high static pressure. The power of the fan is designed which does not have overloading. The guide vanes are used to eliminate the swirl imparted to air by the fan blades. Hence it can be at the outlet side in some designs [33].

5.2.2 Production of Duct Fan

A ducted fan consists of the following parts which are screws (Figure 5.15), bolts (Figure 5.16), hub (Figure 5.17). They produce the torque to balance main rotor's produced torque. A brushless electric engine (Figure 5.22) is also used for rotating the propeller (Figure 5.18).

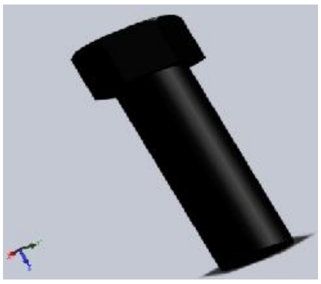

Figure 5. 15 Screw

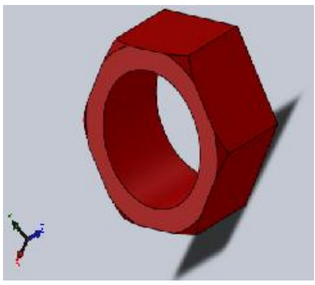

Figure 5. 16 Bolt

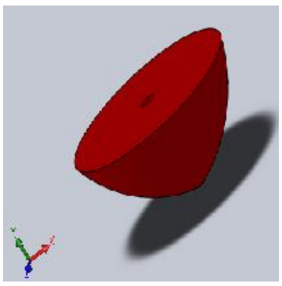

Figure 5. 17 Hub

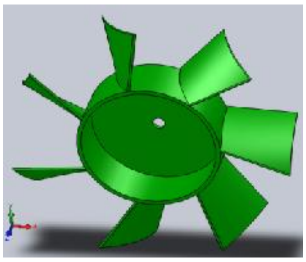

Figure 5. 18 Propeller

Figure 5. 19 Tail Shaft

Figure 5. 20 Brass Metal Strip

Brass metal strip (Figure 5.20) is used to fix the ducted fan to helicopter tail shaft (Figure 5.19). Duct fan case (Figure 5.23) is assembled to brass metal. Electric engine shaft is elongated with shaft (Figure 5.21).

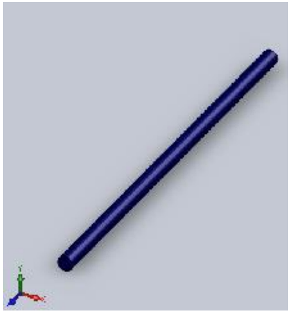

Figure 5. 21 Shaft

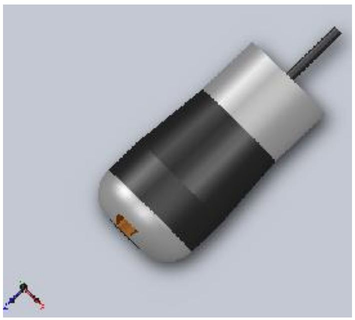

Figure 5. 22 Engine

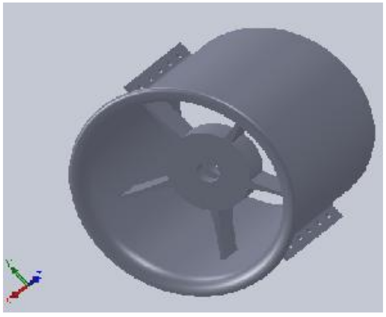

Figure 5. 23 Duct Fan Case

5.2.3 Performance and Thrust Calculation with Static Tapping Systems

Two setups have been prepared for experiments. These setups are used for the static tapping (Figure 5.26 and Figure 5.27) and spring system (Figure 5.32) for 70 mm duct fan (Figure 5.24) which has features in the table 5.2.

Table 5. 2 Features of Duct Fan

Features of Duct fan	**Values**
Engine	4800 (rpm/V) brushless engine
Engine Power	290 Watt
Battery	11.1 V lipo -3 cell -2300 mAh
Size	70 mm diameter
Hub diameter	29.5 mm
Weight	130 gr
Length	60 mm
Blade number	6
Stator number	4
Electronic Speed Control	30 amp esc (BEC) programmable

Figure 5. 24 Duct Fan Systems

Figure 5. 25 Remote Control

The duct fan has been placed in the pipe (Figure 5.27). The duct fan is controlled by a remote control system (Figure 5.25). Static tapping holes have been drilled on the pipe. Mass flow rate has same along the duct. Duct fan's cross section area has not been change along the duct. Static pressure has been measured with alcoholmeter by static tapping (Figure 5.26). Then, the pressure has been multiplied with duct fan cross sectional area and obtained thrust from this system. Air velocity is detected on the outlet ducted fan by anemometer. Cycle of brushless electric engine has been determined by tachometer (Figure 5.28).

Figure 5. 26 Static Tapping 3D View

Figure 5. 27 Static Tapping Back View

5.2.3.1 Equations for Static Tapping System

a) Air Density

$P_{atm} = 690\ \text{mmHg}$ T=22 ºC $R = 287$

$T = 273 + 22 = 295$

Atmospheric pressure has been measured as a column of mercury in the laboratory conditions. Air density has been found with equation (5.4).

$$P_{atm} = \rho gh \tag{5.3}$$

$$= 13600 \times 9{,}81 \times 0{,}69$$

$$= 92\ \text{kpa}$$

$$P_{atm} = \rho RT \tag{5.4}$$

$$\rho = \frac{P_{atm}}{RT}$$

$$\rho = \frac{92}{0{,}287 \times 295}$$

$$\rho = 1{,}12$$

b) Mean Velocity

Mean velocity has been calculated with volumetric flow rate over duct fan area with equation (5.5). Volumetric flow rate is measured with anemometer (Figure 5.29).

$$U_{mean} = \frac{Q}{A} \tag{5.5}$$

$A=000385m^2$

Figure 5. 28 Tachometer

Figure 5. 29 Anemometer

c) Determine Nature of the Flow

Mach number has been found mean velocity over speed of sound in equation (5.6).

a=348 m/s

$$M = \frac{U_{maen}}{a} \tag{5.6}$$

The flow has been accepted incompressible due to less than 0.2 Mach number [35]. Some researcher accepts 0.3 as the limit for incompressibility [36].

d) Reynolds Numbers

Reynolds numbers has been found with equation (5.7).

$\mu = 1.705 \times 10^{-6}$

$$Re = \frac{\rho \times U_{mean} \times D}{\mu} \tag{5.7}$$

e) *f* Friction Factor

Friction factor *f* has been calculated by considering the flow as turbulent.

$$f = \frac{0.079}{Re^{1/4}} \tag{5.8}$$

f) Calculations the Loss

Duct fan is placed inside a pipe (Figure 5.30), so some losses have been created due to friction. H_{loss} has been calculated equation (5.9). Darcy-weisbach friction factor has been computed on equation (5.8).

$$H_{loss} = 4 \times f \times \left(\frac{L}{D} \times \frac{{U_{mean}}^2}{2 \times g} \right) \qquad (5.9)$$

g) General Equations

Bernoulli equations are used to find pressure differences between inlet and outlet duct fan. Due to nature of incompressible flow, the Bernoulli equation has been applied to find pressure differences.

$$\frac{P_1}{\rho g} + \frac{{U_1}^2}{2g} + z_1 + H_{fan} = \frac{P_2}{\rho g} + \frac{{U_2}^2}{2g} + z_2 + H_{loss} \qquad (5.10)$$

Air density (ρ) is not change any measure in the pipe. This has been found equation (5.6). Due to both unchanged air density and cross sectional area, air velocity has been same everywhere in the pipe. So the continuity equation is;

$$\rho . U_1 . A_1 = \rho . U_2 . A_2 \qquad (5.11.a)$$

$$A_1 = A_2$$

$$\rho . U_1 . A_1 = \rho . U_2 . A_1 \qquad (5.11.b)$$

$$U_1 = U_2 \qquad (5.11.c)$$

z_1 and z_2 have the same vertical height, so the equation (5.10) will be reduced to the following equation.

$$\frac{P_1}{\rho g} + H_{fan} = \frac{P_2}{\rho g} + H_{loss} \qquad (5.12.a)$$

$$\Delta P = \rho . g . (H_{fan} - H_{loss}) \qquad (5.12.b)$$

The parameters of the experiment such as V_{out} , H_{fan} , RPM , Q have been measured with anemometer, tachometer and alcoholmeter. Other parameters on the Table 5.3 have been calculated with above equations.

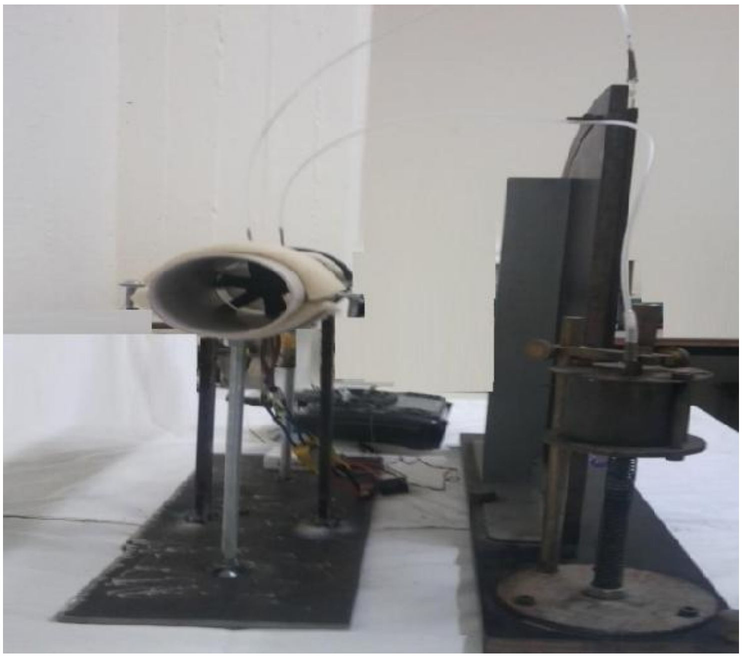

Figure 5. 30 Static Tapping System Left View

h) Thrust Calculation

Thrust is calculated static pressure multiply cross sectional area (Figure 5.31).

$$T_{static\ pressure} = \Delta P \times A \qquad (5.13)$$

Figure 5. 31 Duct Fan Systems in Pipe

5.2.4 Thrust Calculation with Spring Systems

Another thrust calculation system has been designed as a spring system (Figure 5.32). In this system, the trust created by duct fan is measured with a spring and pulley system. First and final lengths of spring are measured and the spring coefficient is described. Then the static thrust has been calculated.

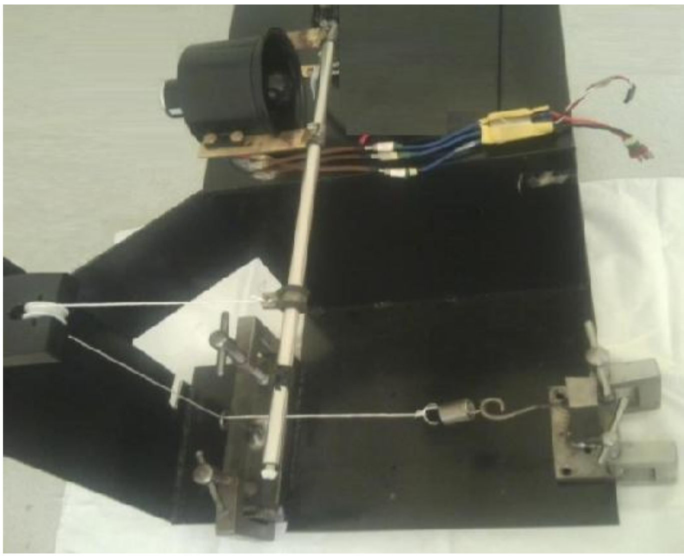

Figure 5. 32 Spring System

5.2.4.1 Equations for Spring Systems

a) Determination of Spring Constant

Spring has been fixed to a flat plate. First length of spring has been measured and recorded with digital compass (Figure 5.33). A weight has been hanged on to spring then the length of spring has been measured and recorded. When weight has been divided to differences of between two measures, spring coefficient has been found.

$L_f = 0{,}02545$

$x = L_e - L_f$

Figure 5. 33 Digital Compass

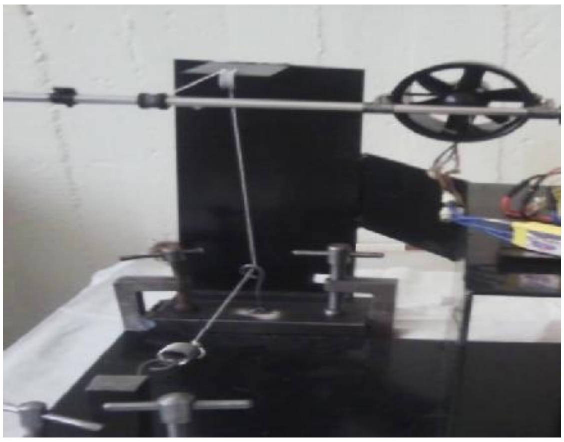

Figure 5. 34 Spring System Front Side

b) Thrust Calculation

Force has been calculated with multiplication of differences between first length of spring and last length of spring. Spring is clearly shown in the figure 5.35.

$$F_{spring} = k_{spring}.x \tag{5.14}$$

Many values have been calculated and given on the Table 5.4 according to various RPM.

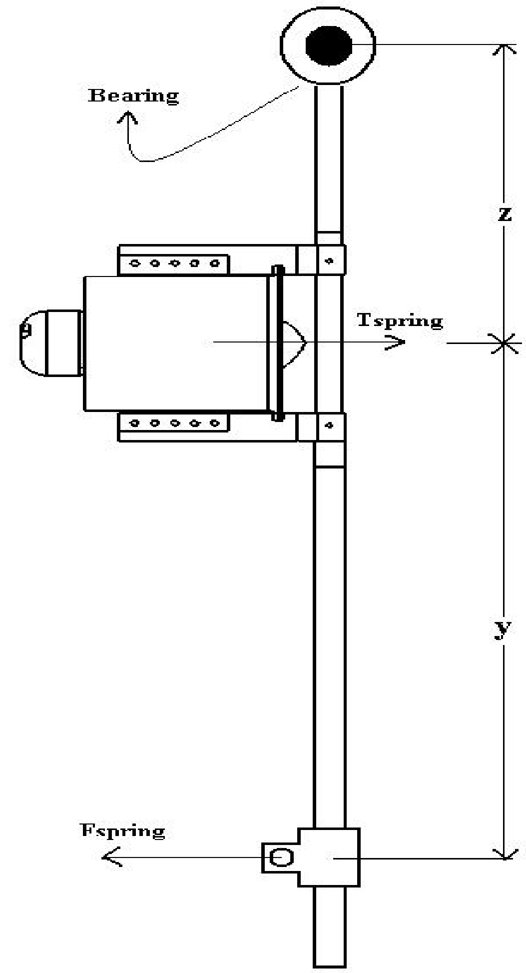

Figure 5. 35 Schematics representation of Spring System

$$T_{spring} . z - F_{spring} . (y + z) = 0 \quad (5.15)$$

y=0.175

z=0.125

Thrust is calculated using moment rule. It is shown in the figure 5.35. T_{spring} has been found with the equation 5.15.

Table 5. 3 Test Results for Static Tapping Systems

RPM	Q m3/h	Duct Area	Flow rate kg/s	Flow rate m3/s	U mean	Reynold	Mach Number	Density Air	*f*	H loss	DELTA P	Static trust
4800	**82**	0,003848	0,025511	0,022777	5,9188	237689,02	0,017008	1,12	0,003	0,0511	31,3050	**0,1205**
5500	**95**	0,003848	0,029555	0,026388	6,8572	275371,43	0,019704	1,12	0,003	0,0661	41,8988	**0,1612**
6500	**119**	0,003848	0,037022	0,033055	8,5895	344938,95	0,024682	1,12	0,003	0,0980	59,0116	**0,2271**
8500	**153**	0,003848	0,0476	0,0425	11,0437	443492,94	0,031734	1,12	0,003	0,1522	76,7346	**0,2953**
9000	**157**	0,003848	0,048844	0,043611	11,3324	455087,53	0,032564	1,12	0,003	0,1592	97,3722	**0,3747**
10000	**178**	0,003848	0,055377	0,049444	12,8482	515959,11	0,036920	1,12	0,002	0,1984	109,997	**0,4233**
11000	**195**	0,003848	0,060666	0,054166	14,0753	565236,10	0,040446	1,12	0,002	0,2327	138,694	**0,5337**
12000	**216**	0,003848	0,0672	0,06	15,5911	626107,68	0,044802	1,12	0,002	0,2783	158,658	**0,6106**
13800	**241**	0,003848	0,074977	0,066944	17,3956	698573,85	0,049987	1,12	0,002	0,3371	208,979	**0,8042**
15000	**268**	0,003848	0,083377	0,074444	19,3445	776837,31	0,055587	1,12	0,002	0,4060	242,815	**0,9344**
15750	**286**	0,003848	0,088977	0,079444	20,6438	829012,95	0,059321	1,12	0,002	0,4549	293,911	**1,1311**
16750	**294**	0,003848	0,091466	0,081666	21,2212	852202,12	0,060980	1,12	0,002	0,4774	362,777	**1,3961**
17500	**309**	0,003848	0,096133	0,085833	22,3040	895681,82	0,064091	1,12	0,002	0,5208	390,760	**1,5038**
18000	**330**	0,003848	0,102666	0,091666	23,8198	956553,40	0,068447	1,12	0,002	0,5844	401,471	**1,5450**
20500	**371**	0,003848	0,115422	0,103055	26,7792	1075397,9	0,076951	1,12	0,002	0,7173	532,303	**2,0485**
24200	**418**	0,003848	0,130044	0,116111	30,1717	1211634,3	0,086700	1,12	0,002	0,8838	699,739	**2,6928**
25200	**438**	0,003848	0,136266	0,121666	31,6153	1269607,2	0,090848	1,12	0,002	0,9591	795,852	**3,0627**
26400	**466**	0,003848	0,144977	0,129444	33,6364	1350769,3	0,096656	1,12	0,002	1,0690	857,861	**3,3013**
27600	**492**	0,003848	0,153066	0,136666	35,5131	1426134,1	0,102049	1,12	0,002	1,1755	943,675	**3,6316**
29400	**560**	0,003848	0,174222	0,155555	40,4214	1623242,1	0,116153	1,12	0,002	1,4745	1045,78	**4,0245**
31200	**600**	0,003848	0,186666	0,166666	43,3087	1739188,0	0,124450	1,12	0,002	1,6637	1125,11	**4,3298**
34800	**680**	0,003848	0,211555	0,188888	49,0832	1971079,7	0,141043	1,12	0,002	2,0711	1407,05	**5,4148**
37000	**745**	0,003848	0,231777	0,206944	53,7750	2159491,7	0,154525	1,12	0,002	2,4299	1614,34	**6,2125**

Table 5. 4 Test Results for Spring System

RPM	First Length	End length	spring thrust	thrust with adding Friction force
4800	30,2	30,55	0,087906	0,118906
5500	30,2	30,7	0,12558	0,15658
6500	30,2	30,95	0,18837	0,21937
8500	30,2	31,25	0,263718	0,294718
9000	30,2	31,55	0,339066	0,370066
10000	30,2	31,74	0,3867864	0,4177864
11000	30,2	32,17	0,4947852	0,5257852
12000	30,2	32,48	0,5726448	0,6036448
13800	30,2	33,24	0,7635264	0,7945264
15000	30,2	33,8	0,904176	0,935176
15750	30,2	34,53	1,0875228	1,1185228
16750	30,2	35,45	1,31859	1,34959
17500	30,2	35,95	1,44417	1,47517
18000	30,2	36,45	1,56975	1,60075
20500	30,2	37,9	1,933932	1,964932
24200	30,2	41,1	2,737644	2,768644
25200	30,2	42	2,963688	2,994688
26400	30,2	43,2	3,26508	3,29608
27600	30,2	44,3	3,541356	3,572356
29400	30,2	46	3,968328	3,999328
31200	30,2	47,2	4,26972	4,30072
34800	30,2	51,4	5,324592	5,355592
37000	30,2	54,7	6,15342	6,18442

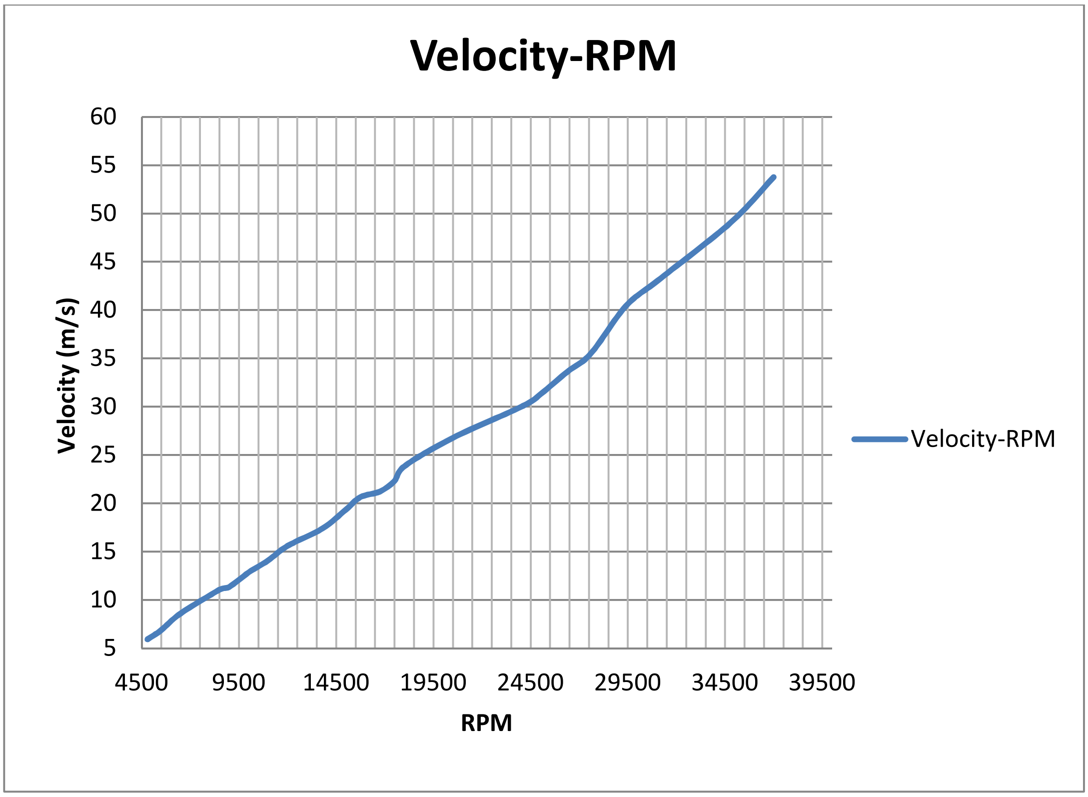

Figure 5. 36 Velocity and RPM Diagram of Ducted Fan (70 mm diameter) Using Static Tapping System.

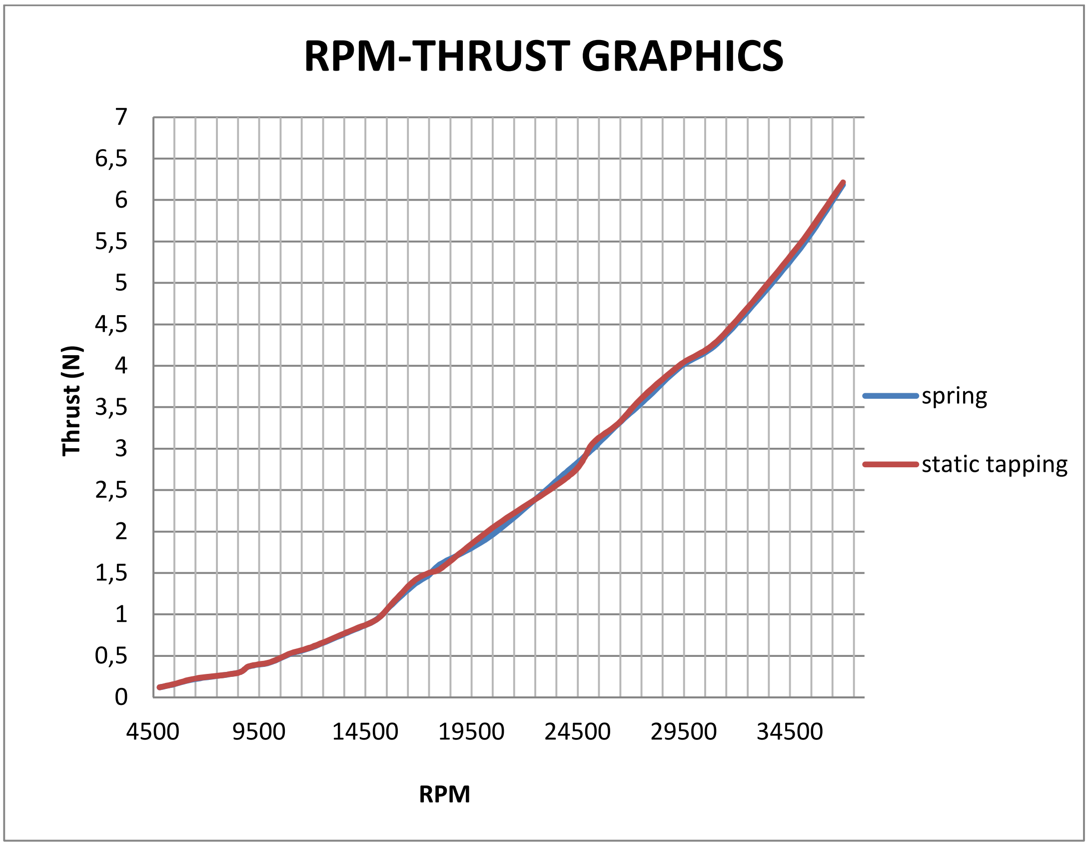

Figure 5. 37 Comparing Thrust between Spring System and Static Tapping.

5.2.5 Validations of These Systems

The determination of the produced trusts of a duct fan in various speeds and RPMs has been achieved in two experimental approaches. Applied methods have the similar results.

Two methods are compared in each other. Moreover error rate has been calculated according to two methods. RPM and error rate have direct relationships (Table 5.4). Velocity-RPM diagram for this duct fan is obtained (Figure 5.36) and it has been also observed that Trust-RPM follows each others at low speed but accuracy will be down at high speeds (Figure 5.37).

5.2.6 Assembling the Helicopter

The produced ducted fan is assembled to helicopter tail shaft (Figure 5.38). Because of the ducted fan is plastic and using brass metal, new system is lighter than helicopter tail rotor systems. Duct fan assembly is shown in the figure 5.38, figure 5.39 and 5.40 show the side views.

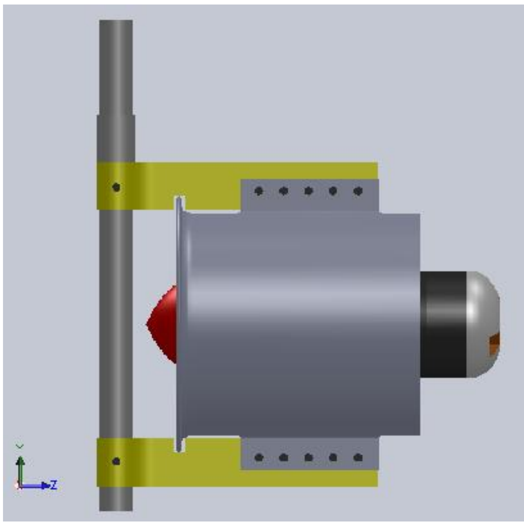

Figure 5. 38 Ducted Fan Full Assemble 1

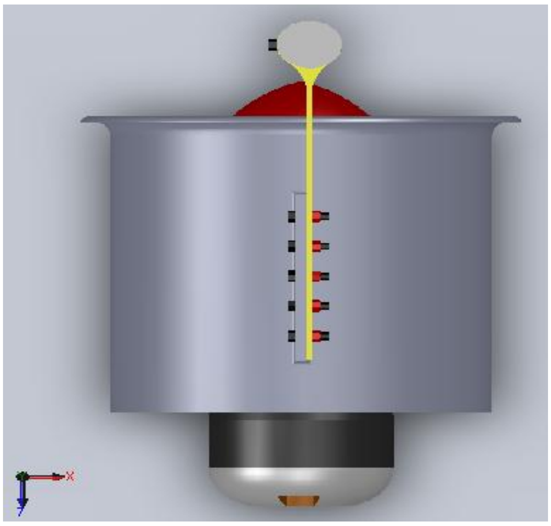

Figure 5. 39 Ducted Fan Full Assemble 2

Ducted fan assembly is shown in the figure 5.41 as transparent.

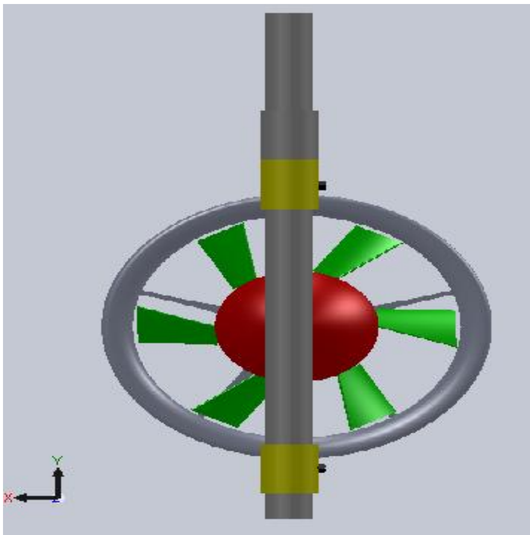
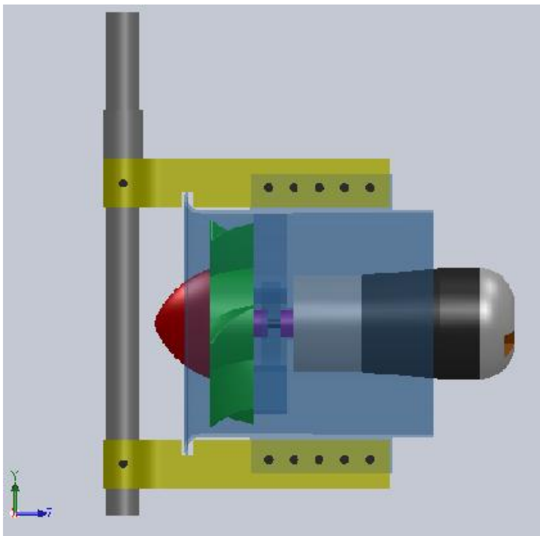

Figure 5. 40 Ducted Fan Full Assemble 3 **Figure 5. 41** Ducted Fan Full Assemble 4

Full assemble of ducted fan is shown in the figure 5.42.

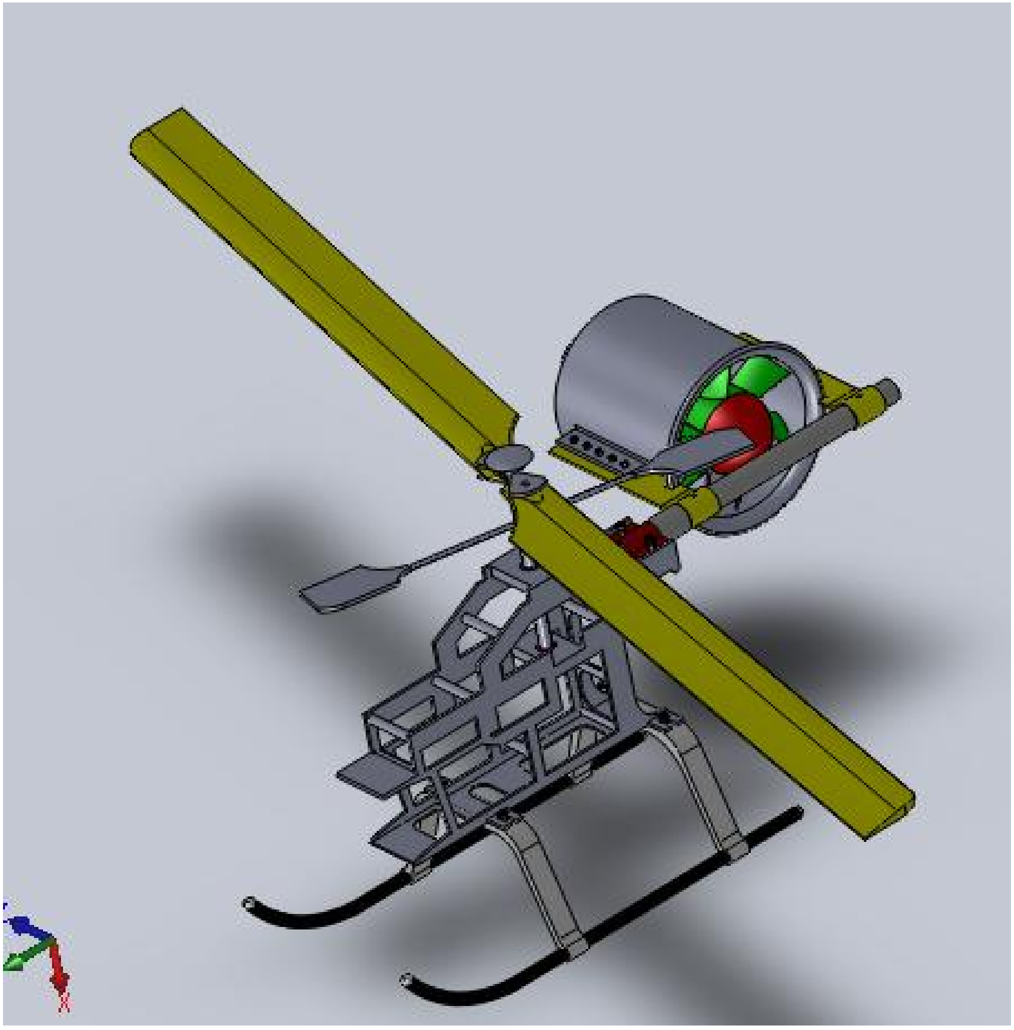

Figure 5. 42 Ducted Fan Full Assemble to Helicopter Tail Shaft

5.3 CASE STUDY

Aim of this thesis is to redesign a helicopter without tail rotor. In this scope, some of improvements are done. For example, tail length is reduced and tail weight is decreased. Ducted fan is used to balance the torque produced by main rotor.

Tail rotor's produced thrust is found with torque meter system. This thrust's produced torque on the main rotor shaft is found with moment rule and then the ducted fan is placed to tail according to ducted fan's produced thrust.

Some of test and experiment are performed for determine the ducted fan's thrust. Static tapping and spring system are used for this. The thrust calculation methods almost gave similar results. Thrust values are calculated from the measured RPM and velocity. Maximum and minimum RPM were 4800-37000 according to motor capacity. The parameters are given for the used system as follows:

α is angle of attack.
∅ is flow angle.
θ is pitch angle=45º.
B is blade number=6
c is chord length=0.015m
C_L is lift coefficient=0.56
C_D is drag coefficient=0.33
r_p is radious of propeller=0.016m
N is revolutions per minute

$$V_{angular} = \frac{2\pi N r_p}{60} \tag{5.16}$$

Flow angle is calculated below,

$$\emptyset = \arctan\left(\frac{V_{axial}}{V_{angular}}\right) \tag{5.17}$$

$$\alpha = \theta - \emptyset \tag{5.18}$$

Angle of attack is found as 20.5º.

$V_{angular}$ is found using N and r_p according to equation 5.16. Flow angle is determined from V_{axial} and $V_{angular}$ with equation 5.17. Lift and drag coefficient is also calculated from the angle of attack on these theories. Lift and drag coefficients are taken from figure 5.43 and figure 5.44 [36]. Thrust is calculated theoretically with blade element equations (3.7) to validate these thrust calculation systems. Momentum theory is also used, while thrust is calculated with static tapping system in the equation (5.13). It is seen that the equation is same equation with (3.3).

$$\Delta T = \frac{1}{2}\rho V_{result}^2 c(C_L \cos(\emptyset) - C_D \sin(\emptyset))Bdr \qquad (3.7)$$

$$T = (p^- - p^+)A \qquad (3.3)$$

Theoretically and experimental results are nearly same. It can be seen on the table.

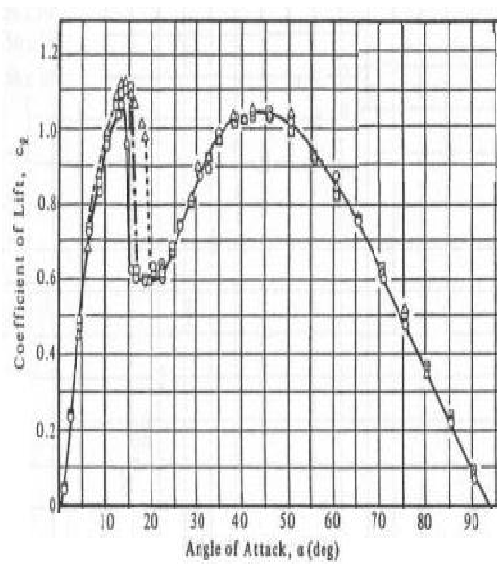

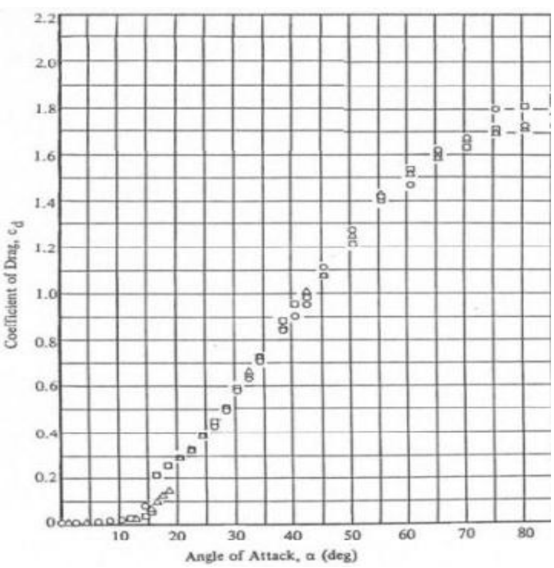

Figure 5. 43a Lift Coefficient of Blade **Figure 5. 44** Drag Coefficient of Blade [36]

Table 5. 5 Comparison of the Theoretical and Experimental Results

RPM	Theoretical Results	Experimental Results		Percentage of Error rate BET & STS	Percentage of Error rate BET & SS
	Blade element thrust (BET)	Static tapping thrust(using momentum theory) (STS)	Spring thrust (SS)		
4800	0,1103	0,1205	0,1189	8,4390	7,211579
5500	0,1444	0,1612	0,1566	10,4386	7,796015
6500	0,1998	0,2271	0,2194	12,0110	8,910516
8500	0,3235	0,2953	0,2947	-9,5483	-9,76459
9000	0,3870	0,3747	0,3701	-3,2826	-4,57594
10000	0,4766	0,4233	0,4178	-12,6008	-14,0868
11000	0,5769	0,5337	0,5258	-8,0868	-9,71381
12000	0,6853	0,6106	0,6036	-12,2273	-13,5204
13800	0,9110	0,8042	0,7945	-13,2816	-14,6609
15000	1,0733	0,9344	0,9352	-14,8652	-14,7698
15750	1,1805	1,1311	1,1185	-4,3648	-5,5383
16750	1,3422	1,3961	1,3496	3,8622	0,549056
17500	1,4617	1,5038	1,4752	2,7989	0,912437
18000	1,5408	1,5450	1,6008	0,2712	3,744495
20500	2,0014	2,0485	1,9649	2,2978	-1,85747
24200	2,8101	2,6928	2,7686	-4,3572	-1,49842
25200	3,0452	3,0627	2,9947	0,5714	-1,68672
26400	3,3349	3,3013	3,2961	-1,0163	-1,17625
27600	3,6377	3,6316	3,5724	-0,1677	-1,82888
29400	4,0832	4,0245	3,9993	-1,4576	-2,09615
31200	4,5986	4,3298	4,3007	-6,2088	-6,92698
34800	5,7038	5,4148	5,3556	-5,3363	-6,50083
37000	6,4170	6,2125	6,1844	-3,2913	-3,76026

At the end of the study, the required torque is obtained by ducted fan on the sufficient length. New design helicopter is lighter than others due to without tail rotor system and mechanism.

CHAPTER 6

RESULTS AND DISCUSSSION

1. Measurement of the created torque

The created torque of main rotor is measured with torque meter system. This system has given some errors. Yarn is used to hang the weights. Measurement weight is decreased between 3 and 5 grams due to using yarn. Friction factor of bearing has also an importance. Because of this, a correction value is added to the systems as 0.031N friction force.

2. The ducted fan

In this thesis, the thrust is calculated from blade element theory. Two types of experiments are applied to ducted fan for determination of the thrust. They have been compared. Results have a average values of % -2,5827 (Percentage of error rate BET and STS) and -3,68863 (Percentage of error rate BET and SS) difference between theories and experiments. Reasons of these differences can be environment conditions like temperature, pressure, humidity and using equipment. The possible reasons are indicated below;

a. Experimental

1. In the theories, all of conditions accept an ideal condition like room temperature is 24 C^{o} and pressure is 1 atm. Although the measurement conditions are different from ideal conditions due to environmental effects. So the results can be different.

2. Electric engine and lithium polymer battery is used to drive the duct fan. The difference can be occurred due to lithium polymer battery life which is changed with time. So we have no idea about time of flight at a constant velocity.

b. Theoretical

1. Although boundary layer created on the surfaces, It is assumed that the boundary layer didn't occur in the pipe. So the experimental and theoretical results have some differences as much as from 2,58 to 3,69% according to the experimental methods.

CHAPTER 7

CONCLUSIONS

In this thesis, helicopter tail rotor concept is changed with ducted fan system. Helicopter became more compact than old designs. In this way the weight of helicopter may be decreased. Some of tail rotor failure is eliminated due to removed tail rotor gear and transmission system.

The tail rotor produced thrust is obtain from duct fan system. Duct fan produced thrust is measured some of thrust measurement systems like static tapping system and spring system. When the results of thrust measurement are examined, it is seen that the measurement thrust is almost same with two different systems.

Blade element and momentum theory are used to validate these measurement thrust. When these theories are applied the duct fan compressor, the theoretical results are seen that they are similar with experimental results.

The needed thrust is provided to balance main rotors produced torque of main rotor with the ducted fan. Duct fan is successfully adapted to helicopter. The new design helicopter is tested to see balancing the main rotors produced torque. The duct fan is performed its mission according to aim of thesis.

The values in the table 5.5 are obtained according to angle of attack and other specifications. There isn't any optimization for case study. In the future works, the angle of attack, velocity and RPM can be optimized according to geometrical properties of propeller.

LIST OF REFERENCES

[1] J. Gordon Leishman, (2000). Principle of helicopter aerodynamics, Cambridge Univesity press.

[2] Historical information about helicopter. 2002. www.schools-wikipedia.org/ wp/ h/Helicopter.htm 24.04.2012

[3] Lynn Townsend White, Jr. (1961). Eilmer of Malmesbury, an Eleventh Century Aviator: A Case Study of Technological Innovation, Its Context and Tradition, *Technology and Culture* 2 (2), p. 97-111.

[4] Wilkins, John. (1802). Concerning Mechanicall Powers and Motions, London 1648, 204, vol. II, 201

[5] Sergio Salazar-Cruz, Rogeli Lozano, Juan Escaren'o. (2009). Stabilization and nonlinear control for a novel trirotor mini-aircraft, *Control Engineering Practice* 17 886–894.

[6] Song Yanguo, Wang Huanjin. (2009). Design of Flight Control System for a Small Unmanned Tilt Rotor Aircraft, *Chinese Journal of Aeronautics* 22 250-256.

[7] Kemao Peng, Guowei Cai , Ben M.Chen, Miaobo Dong, Kai Yew Lum, Tong H. Lee. (2009). Design and implementation of an autonomous flight control law for a UAV Helicopter, *Automatica* 45 2333_2338.

[8] A.T. Conlisk, (2001). Modern helicopter rotor aerodynamics, *Progress in Aerospace Sciences* 37 419–476.

[9] Jenping Chen, Roberts S. Webster, Gary J. Skoch, Gregory P. Herrick, Michael D. Hathaway, (2005). Technology for Stabilizing the Compression System of a US Army Helicopter Gas Turbine Engine: Validation of Unsteady Simulations, *American Helicopter Society 61st Annual Forum, Grapevine, TX,* June 1-3.

[10] Guowei Cai, Lin Feng, Ben M. Chen , Tong H. Lee. (2008). Systematic design methodology and construction of UAV helicopters, *Mechatronics* 18 545–558.

[11] Peter G. Hamel and Jiirgen Kaletka, (1997). Advanced in rotorcraft system identification, *Prog. Aerospace* Sci. Vol. 33, pp. 259-284.

[12] M. Balasko, E. Svab, Gy. Molnar, I. (2005). Veres Classification ofdef ects in honeycomb composite structure of helicopter rotor blades, *Nuclear Instruments and Methods in Physics Research* A 542 45–51.

[13] N.J. Lourenço, (2005). C.F.A. Von Dollinger, M.L.A. Grac, P.P. de Campos Failure analysis of the main rotor grip of a civil helicopter, *Engineering Failure Analysis* 12 43–47.

[14] Nathan A. Miller and Donald L. Kunz. (2008). A comparison of main rotor smoothing adjustments using linear and neural network algorithms, *Journal of Sound and Vibration* 311 991–1003.

[15] D. McLeana and H. Matsuda. (1998). Helicopter station-keeping: comparing LQR, fuzzy-logic and neural-net controllers, *Engineering Applications of Artificial Intelligence* 11 411-418.

[16] G. Heredia, A. Ollero, M. Bejar, R. Mahtani. (2008). Sensor and actuator fault detection in small autonomous helicopters, *Mechatronics* 18 90–99.

[17] M. Balasko, I. Veres, Gy. Molnar, Zs. Balasko, E. Svab. (2004). Composite structure of helicopter rotor blades studied by neutron- and X-ray radiography, *Physica* B 350 107–109.

[18] M. K. Rwigema. (2010). propeller blade element momentum theory with vortex wake deflection, *In ICAS, 27th international congress of the aeronautical sciences,* France, ICAS 2010-2.3.4.

[19] Quentin R. Wald. (2006).the aerodynamics of propellers, *Progress in Aerospace Sciences* 42 85–128.

[20] Jean-Jacques Chattot. (2009). Effects of blade tip modifications on wind turbine performance using vortex model, *Computers & Fluids* 38 1405–1410.

[21] E. Ritschl, R. Theiner, D. Hanus. (2003). Inlet Channel for a Ducted Fan Propulsion System of a Light Aircraft, *Acta Polytechnica* Vol. 43 No 6.

[22] Michael R. Mendelhall and Selden B. Spangler. (1970). Theoretical study of ducted fan performance, National aeronautics and space administration contractor report, *NASA CR-1494*.

[23] Thong Q.Dang and PeterR.Bushnell. (2009). Aerodynamics of cross-flow fans and their application to aircraft propulsion and flow control, *Progress in Aerospace Sciences* 45 1–29.

[24] J. A. Lieser, D. Lohmann, C. H. Rohardt. (1997) Aeroacoustic Design of a 6-Bladed Propeller, *Aerospace Science and Technology*, nº 6, 381-389.

[25] David Zelman. (2006). Technical Research Report: The Helicopter, University of California, *Santa Barbara College of Engineering*.

[26] Helicopter works principles. 2001. www.helicopterlawyers.com/how_ helicopters_work.html. 20.04.2012

[27] Rotor configuration. 1997. www.helis.com/howflies/rotconf2.php. 17.04.2012

[28] Department of the Navy Chief of Naval Air Training Naval Air Station Corpus Christi. 2000. Introduction to Helicopter Aerodynamics Workbook. Texas 78419-5100.

[29] J. SEDDON. 1990. Basic Helicopter Aerodynamics, BSP Professional Books, ISBN 0-632-02032-6.

[30] Tony Giampaolo. 2010. Compressor Handbook: Principles and Practice, TJ990-G53 2010.

[31] Electrical Energy Equipment: Compressors and Compressed Air Systems, Energy Efficiency Guide for Industry in Asia. 2006. www.energyefficiencyasia.org. 05.05.2012

[32] National aeronautics and space administration. 2008. www.grc.nasa.gov/ WWW /k-12/airplane/caxial.html. 23.03.2012

[33] Basic Guidelines For Plastic Conversion Of Metal Axial Flow Fans. 2003 BASF Corporation. New Jersey 07828-1234

[34] H. Jing, L. Ru, H. Yaling, Q. Zhiguo. (2007). Solutions for variable density low Mach number flows with compressible pressure-based algorithm, *Applied Thermal Engineering* 27 2104–2112.

[35] Almegren, A.S., Bell J.B., Rendleman C.A., Zingale M. (2006). Low mach number modeling of type Ia supernovae. 1.Hydrodynamics, *The Astrophysical Journal*, 637:922–936.

[36] Airfoils at High Angle of Attack. 2003. www.aerospaceweb.org/question/ airfoils/q0150b.shtml. 15.04.2012